

1 **Septin-dependent assembly of the exocyst is essential for plant infection by**
2 ***Magnaporthe oryzae***

3
4 **Yogesh K. Gupta^{1,2}, Yasin F. Dagdas^{1,2}, Ana-Lilia Martinez-Rocha^{1†}, Michael J. Kershaw¹,**
5 **George R. Littlejohn¹, Lauren S. Ryder¹, Jan Sklenar², Frank Menke² and Nicholas J.**
6 **Talbot^{1*}**

7
8
9
10
11
12
13
14 ¹ School of Biosciences, University of Exeter, Exeter, EX4 4QD, UK

15 ² The Sainsbury Laboratory, Norwich Research Park, Norwich, NR4 7UH, UK

16 [†] *Present address:* Department of Molecular Phytopathology and Genetics, University of
17 Hamburg, Biozentrum Klein Flottbek, D-22609 Hamburg, Germany

18 * *Corresponding Author:* N.J.Talbot@exeter.ac.uk

19

20 *Magnaporthe oryzae* is the causal agent of rice blast disease, the most devastating disease of
21 cultivated rice and a continuing threat to global food security. To cause disease, the fungus
22 elaborates a specialized infection cell called an appressorium, which breaches the cuticle of the
23 rice leaf, allowing the fungus entry to plant tissue. Here, we show that the exocyst complex
24 localises to the tips of growing hyphae during vegetative growth, ahead of the Spitzenkörper, and
25 is required for polarised exocytosis. However, during infection-related development the exocyst
26 specifically assembles in the appressorium at the point of plant infection. The exocyst
27 components, Sec3, Sec5, Sec6, Sec8, Sec15, Exo70 and Exo84 localize specifically in a ring
28 formation at the appressorium pore. Targeted gene deletion, or conditional mutation, of genes
29 encoding exocyst components leads to impaired plant infection. We demonstrate that
30 organisation of the exocyst complex at the appressorium pore is a septin-dependent process,
31 which also requires regulated synthesis of reactive oxygen species by the NoxR-dependent Nox2
32 NADPH oxidase complex. We conclude that septin-mediated assembly of the exocyst is
33 necessary for appressorium re-polarisation and host cell invasion.

34

35 **INTRODUCTION**

36 *Magnaporthe oryzae* is a filamentous fungus and the causal agent of rice blast disease. Each
37 year, rice blast disease causes up to 18% yield losses and recurrent epidemics occur in all rice-
38 growing regions of the world (Wilson and Talbot, 2009). Understanding the biology of plant
39 infection by *M. oryzae* is therefore critical for development of durable control strategies for blast
40 disease. In order to infect plants, *M. oryzae* develops a specialized infection structure called an
41 appressorium. This dome-shaped cell generates enormous turgor of up to 8.0 MPa to breach the
42 leaf cuticle using a narrow penetration peg that develops from the base of the appressorium (de

43 Jong et al., 1997; Wilson and Talbot, 2009). The fungus subsequently colonizes host epidermal
44 cells and spreads rapidly in plant tissue. Appressorium development occurs in response to the
45 hard, hydrophobic rice leaf surface (Veneault-Fourrey et al., 2006; Saunders et al., 2010). The
46 appressorium generates pressure by accumulating osmolytes, such as glycerol, to very high
47 concentrations and uses autophagic cell death of the conidium to re-cycle cellular components to
48 the developing appressorium (Kershaw and Talbot, 2009; Veneault-Fourrey et al., 2006).

49 Recently, it has been shown that septins assemble into a heteromeric ring at the point of
50 plant infection, called the appressorium pore, where they scaffold a toroidal F-actin network at
51 the base of the appressorium (Dagdas et al., 2012). Septin GTPases act as a diffusion barrier to
52 localize Bin-Amphiphysin-Rvs (BAR)-domain proteins, required for generation of membrane
53 curvature and protrusion of the penetration peg to rupture the leaf cuticle (Dagdas et al., 2012).
54 Septin-mediated re-orientation of F-actin is controlled by the action of NADPH oxidases (Nox)
55 which generate reactive oxygen species in the appressorium (Ryder et al., 2013). The Nox2–
56 NoxR complex is required for organization of the septin ring and F-actin network at the
57 appressorium pore.

58 During plant infection, pathogenic fungi secrete a repertoire of effector proteins, which
59 are small, secreted proteins, to overcome plant immunity. *M. oryzae* secretes apoplastic effectors
60 which localize at the plant fungal interface, while cytoplasmic effectors are expressed at a
61 specialized plant derived structure called the biotrophic interfacial complex and then delivered
62 into rice cells (Khang et al., 2010). It has recently been shown that the *M. oryzae* exocyst sub-
63 units (Exo70 and Sec5) and the t-SNARE, Sso1 are required for secretion of cytoplasmic
64 effectors (Giraldo et al., 2013; Giraldo and Valent, 2013).

65 In this report, we investigated the organisation and function of the exocyst complex
66 during plant infection by *M. oryzae*. Polarized exocytosis is an essential process in fungi required
67 for cell growth, cell migration and morphogenesis. Secretory vesicles are delivered to the hyphal
68 tip and form a vesicle dense region, called the Spitzenkörper (Read, 2011; Riquelme, 2013;
69 Riquelme et al., 2014; Steinberg, 2007; Sudbery, 2011b). This acts as a vesicle supply centre,
70 directing secretory vesicles for cell wall biogenesis to the hyphal tip (Riquelme et al., 2007;
71 Verdin et al., 2009). The Spitzenkörper, together with the polarisome and exocyst complex, play
72 a crucial role in hyphal tip growth (Sudbery, 2011a; Taheri-Talesh et al., 2008). In the budding
73 yeast *Saccharomyces cerevisiae*, the polarisome complex consists of Pea2, Spa2 and the formin,
74 Bni1, which nucleates F-actin cables to sites of polarized growth (Evangelista et al., 2003; Sagot
75 et al., 2002; Sheu et al., 1998). Post-Golgi secretory vesicles are then delivered to the tip via the
76 Rab GTPase Sec4, which is activated through its guanine nucleotide exchange factor (GEF),
77 Sec2 (Stalder et al., 2013) and binds to the exocyst complex through Sec15 interaction (Salminen
78 and Novick, 1989). The exocyst complex is an evolutionary conserved octameric protein
79 complex, comprising Sec3p, Sec5p, Sec6p, Sec8p, Sec10p, Sec15p, Exo70p and Exo84p
80 required for vesicle docking to the plasma-membrane (Guo et al., 1999; He and Guo, 2009;
81 TerBush et al., 1996). Vesicle fusion to the plasma-membrane then requires soluble N-
82 ethylmaleimide-sensitive factor attachment protein receptors (SNAREs), with v-SNAREs on
83 vesicles and t-SNAREs at the plasma membrane (Novick et al., 2006).

84 Here, we show that the octameric exocyst complex in *M. oryzae* is located at the hyphal
85 tip, ahead of the Spitzenkörper. During initial stages of appressorium development, the exocyst is
86 located at the tips of germ tubes, but then adopts a cortical pattern of localization in the
87 expanding appressorium, before specifically localising to the appressorium pore. We

88 demonstrate that exocyst assembly is dependent on septins, which facilitates cuticle rupture and
89 plant infection by the fungus.

90

91 **RESULTS**

92 **Sub-cellular localization of polarity components in vegetative hyphae of *M. oryzae***

93 To understand the role of the exocyst during polarized, hyphal growth in *M. oryzae*, we
94 visualized a range of polarity markers and each of the predicted exocyst components by tagging
95 them with fluorescent proteins and expressing the functional constructs in *M. oryzae*. We first
96 identified *M. oryzae* homologues of each gene by analysis of the genome sequence of *M. oryzae*
97 (Dean et al., 2005), as shown in Supplemental Table 1. Each gene fusion was expressed under its
98 native promoter in *M. oryzae* with C-terminal fusions of GFP used, except for Snc1, Cdc42,
99 Rac1 and Sec4 where N-terminal GFP tags were generated.

100 We first observed localisation of each of the exocyst components Exo70, Sec15, Sec8,
101 Sec3, Sec6, Exo84, Sec5 and Sec10, in growing hyphae of *M. oryzae*. All exocyst components,
102 except Sec10, localized to a crescent structure at the growing hyphal tip, as shown in Figure 1.
103 We were unable to observe any signal in Sec10-GFP expressing strains of *M. oryzae* (data not
104 shown). This is consistent with a previous finding in *N. crassa*, where a Sec10-GFP fusion could
105 not be localised, even though Sec10 was shown by immuno-precipitation to be part of the
106 exocyst complex (Riquelme et al., 2014). This suggests that there might be a conserved structural
107 impediment to expressing a Sec10-GFP fusion in the related ascomycete species, *M. oryzae* and
108 *N. crassa*. Expression analysis of genes expressing each exocyst component was performed
109 using by SuperSAGE analysis (Soanes et al., 2012) and suggested that *SEC10* is expressed in
110 mycelium grown in complete medium and during appressorium development, albeit at a low

111 level compared with some of the other exocyst components, such as *SEC3* and *SEC15*
112 (Supplemental Figure 1).

113 To investigate location of the Spitzenkörper in *M. oryzae*, we labelled hyphae expressing
114 exocyst-GFP fusions with the lipophilic styryl dye, FM4-64 (Fischer-Parton et al., 2000). The
115 Spitzenkörper appeared as a bright spot in the centre of the apical dome, while the exocyst
116 components formed a surface crescent at the tips of cells (Figure 1, Supplemental Figure 2). Line
117 scans of the fluorescence signals confirmed this separation for each component of the exocyst
118 complex, with only a partial overlap in fluorescence observed, for example, with Sec3
119 (Supplemental Figure 2). In contrast, myosin light chain, Mlc1, localized to a region consistent
120 with the Spitzenkörper (Supplemental Figure 3A). The polarisome component Spa2-GFP also
121 localized as a bright spot at the hyphal tip (Supplemental Figure 3B; Supplemental Movie 1).
122 Fimbrin-GFP localised sub-apically to a cortical collar in growing hyphae (Supplemental Figure
123 3C; Supplemental Movie 2), while other polarity components, Snc1, Sec2, Sec9, Sec4 and Rac1
124 preferentially localized to the tips of growing vegetative hyphae (Supplemental Figure 3D-H and
125 Supplemental Movie 4). GFP-Cdc42 was cortically distributed with strong tip localisation
126 (Supplemental Fig 3I; Supplemental Movie 3). Moreover, Sec2, the putative guanine nucleotide
127 exchange factor (GEF) for Sec4, was tip localised, often appearing slightly sub-apical to the
128 Spitzenkörper (Supplemental Fig 4) We conclude that the exocyst forms a complex at the very
129 apex of hyphal tips of *M. oryzae* that is distinct from the Spitzenkörper.

130 In order to understand the composition of the exocyst complex, Sec6-GFP and Exo84-
131 GFP were immuno-precipitated from hyphal protein extracts and liquid chromatography-tandem
132 mass spectrometry (LC-MS/MS) performed to identify unique peptides. Mass-spectrometry data
133 was aligned with the predicted set of *M. oryzae* proteins and parameters set to 95% confidence

134 for protein match and a minimum of two unique peptide matches with 95% confidence. All
135 seven of the remaining exocyst subunits were identified by co-immunoprecipitation with Sec6
136 and Exo84, as shown in Table 1, consistent with the predicted octameric nature of the complex.
137 Interestingly, Sec10 was always observed in co-immunoprecipitation experiments with both
138 Sec6 and Exo84 and we conclude that it forms part of the octameric exocyst complex. However,
139 our inability to co-localise Sec10 in live cell imaging studies does not preclude the possibility
140 that it is not always associated with the rest of the sub-units, or is present in only a sub-set of
141 complexes. We also identified additional interacting proteins, including all four core septin
142 GTPases, actin-binding proteins, Rho-GTPase and the Pmk1 MAPK (Mitogen-activated protein
143 kinase), which is involved in regulation of appressorium development in *M. oryzae* (Xu and
144 Hamer, 1996). The proteins identified are consistent with the exocyst being associated with the
145 polarised tips of fungal hyphae and their predicted function in exocytosis, but also suggested a
146 specific involvement in appressorium-mediated plant infection.

147 **Organisation of the exocyst at the appressorium pore of *M. oryzae***

148 To understand the role of the exocyst components during plant infection, we visualized
149 expression and localisation of exocyst-GFP fusion proteins during a time course of appressorium
150 development. Each exocyst subunit initially localized to tips of germinating conidia and germ-
151 tubes during the early stages of appressorium development, as shown in Figure 2 and
152 Supplemental Figure 5. Once the appressorium formed, we observed exocyst components at the
153 cortex of cells with a punctate distribution (4-8 h). In three-dimensional projections, it was clear
154 that localization was associated with the base of the infection cell at its interface with the
155 underlying surface (Supplemental Movie 6). In mature appressoria (24 h), exocyst components
156 localized to a 4.0 μm diameter ring (± 0.4 , n=50) at the appressorium pore (Figure 2A, 2B and

157 Supplemental Figure 5). This is consistent with the inside edge of the heteromeric septin ring
158 complex, and the toroidal F-actin network that bring about re-polarisation of the appressorium
159 during plant infection (Dagdas et al., 2012). We co-localised F-actin in a strain expressing Sec6-
160 GFP by expression of LifeAct-RFP. Toroidal F-actin co-localised with the exocyst ring
161 extending in a larger, more dispersed network around the appressorium pore (Figure 2C). To
162 investigate the nature of the appressorium pore, we investigated the localization of other polarity
163 components. We found that Sec9-GFP, a putative membrane-bound t-SNARE, localized in
164 puncta around the appressorium pore (Supplemental Figure 6). Similarly, Snc1-GFP (a putative
165 vesicle bound v-SNARE), Fim1-GFP (Fimbrin, an actin-binding protein), Rac1-GFP (a Rho type
166 GTPase) and Cdc42-GFP (a polarity-associated small GTPase) all localized at the centre of the
167 appressorium pore (Supplemental Figure 6). These results are consistent with the appressorium
168 pore acting as an active hub for signalling during re-establishment of polarised growth during
169 plant infection.

170 **Exocyst-dependent secretion at the appressorium pore**

171 To investigate the role of the appressorium pore in polarized exocytosis, we next determined if
172 known pathogenicity determinants are secreted in an exocyst-dependent manner during plant
173 infection. We initially checked secretion of total protein in axenic culture from exocyst mutants
174 $\Delta sec5$ and $\Delta exo70$ and compared this to the isogenic wild type Guy11. In $\Delta sec5$ and $\Delta exo70$
175 there was, respectively, greater than 50% and 60% reduction in secretion of protein compared to
176 Guy11 ($P < 0.01$) (Supplemental Figure 7). We then investigated secretion of a virulence-
177 associated factor. During initiation of plant infection by *M. oryzae* the fungal spore releases
178 spore tip mucilage (STM) to attach itself to the leaf surface (Hamer et al., 1988). This acts as an
179 adhesive and is also secreted from the appressorium to facilitate adhesion to the hydrophobic

180 cuticle. STM can be detected using the lectin concanavalin A conjugated to fluorescein
181 isothiocyanate (FITC) (Hamer *et al.*, 1988). We investigated STM secretion in $\Delta sec5$ and $\Delta exo70$
182 mutants. Spores from $\Delta sec5$ and $\Delta exo70$ mutants were harvested and appressoria allowed to form
183 on hydrophobic borosilicate glass coverslips. Secretion of STM was then observed by FITC-
184 ConA labeling and epifluorescence microscopy, as shown in Figure 3. Spores of Guy11 showed
185 a very strong signal for STM compared to those of $\Delta sec5$ and $\Delta exo70$ mutants both at the tips of
186 germinating conidia and at the base of appressoria (Figure 3A). We observed that 83% and 71%
187 conidia from $\Delta sec5$ and $\Delta exo70$ mutants showed less fluorescence than Guy11, respectively
188 (Figure 3B). Similarly, the fluorescence signal from mature appressoria in exocyst mutants was
189 also significantly reduced ($P < 0.05$) with 80% and 66% of appressoria showing less fluorescence
190 in $\Delta sec5$ and $\Delta exo70$ mutants, respectively, than Guy11.

191 Consistent with impaired secretion, $\Delta sec5$ and $\Delta exo70$ mutants are required for full
192 virulence (Figure 3C and D). We used the susceptible rice (*Oryza sativa*) cultivar Co-39 and
193 found a significant ($P < 0.05$) reduction in the ability of exocyst mutants to cause rice blast disease
194 compared to Guy11 (Figure 3C). Taken together, we conclude that the appressorium pore is an
195 active site of secretion during plant infection.

196

197 **Sec6 is required for exocyst assembly at the appressorium pore**

198 To investigate exocyst function, we attempted to generate targeted gene deletion mutants for all
199 exocyst-encoding genes. All exocyst subunits are essential in yeast, except Sec3, although $\Delta sec3$
200 mutants show severe growth defects (Wiederkehr *et al.*, 2003), while temperature sensitive
201 mutations in exocyst subunits, lead to accumulation of secretory vesicles at the sites of bud tips
202 and the mother bud neck (Novick *et al.*, 1980). In *M. oryzae* only $\Delta sec5$ and $\Delta exo70$ mutants

203 could be generated (Giraldo et al., 2013). We therefore generated a temperature-sensitive mutant
204 of *SEC6*. In yeast, the *sec6-4* mutant grows normally at 25 °C but at non-permissive temperature,
205 37 °C, its growth is severely impaired. Generating a point mutation, L633P, in the *SEC6* coding
206 region leads to the *sec6-4* phenotype (Lamping et al., 2005), so we attempted to target the same
207 region of *M. oryzae SEC6* to generate a temperature-sensitive mutant by allelic replacement. We
208 mutated the Y601P site in the *SEC6* coding region and then introduced the allele into *M. oryzae*
209 by homologous recombination. Putative *sec6^{Y601P}* transformants were selected and showed a
210 growth defect at a semi-restrictive temperature of 29 °C. Growth was restored by subsequent
211 incubation at 24 °C, as shown in Figure 4. Positive transformants were confirmed by DNA
212 sequence analysis of the mutation site (Supplemental Figure 8B). Integration of the selectable
213 maker hygromycin (1.4 kb) was further confirmed by PCR using primers Sec6.TS.2F and
214 Sec6.30.1 (Supplemental Figure 8C and Supplemental Table 2).

215 In budding yeast, conditional mutation of Sec6 causes disassembly of the exocyst
216 complex at 37°C (Songer and Munson, 2009). To test whether the exocyst complex depends on
217 Sec6 for assembly at the appressorium pore, we investigated pore organisation in the *sec6^{Y601P}*
218 mutant. We localized Sec5-GFP and Sec8-GFP in the *sec6^{Y601P}* mutant and found that ring
219 confirmation of the exocyst complex was disrupted at the semi-restrictive temperature of 29 °C,
220 but formed normally at 24 °C (Figure 4B and C). Consistent with loss of exocyst organisation,
221 we found the *sec6^{Y601P}* mutant was significantly reduced (P<0.05) in its ability to cause rice blast
222 disease at 29 °C, but showed normal virulence at 24 °C compared to Guy11 (Figure 4D and E).
223 We also localized exocyst components Exo70, Sec3, Exo84, Sec15 in a *sec6^{Y601P}* mutant and
224 none formed rings at 29 °C (Supplemental Figure 9). Loss of virulence was restored when we
225 complemented the *sec6^{Y601P}* mutant with a functional Sec6-GFP fusion (Supplemental Figure

226 8D). A leaf sheath assay was performed to check growth of invasive hyphae on rice cultivar Co-
227 39. At semi-restrictive temperature, the growth of *sec6*^{Y601P} mutant is restricted in the first rice
228 cell (45 hpi) while Guy11, and complemented strains, invaded up to three rice cells by this time
229 (Supplemental Figure 8D). We conclude that Sec6 is required for core assembly of exocyst
230 subunits at the appressorium pore, which is a necessary pre-requisite for plant infection.

231

232 **Septin-dependent assembly of the exocyst complex**

233 In *M. oryzae* the toroidal F-actin network at the appressorium pore is organised by a
234 heteromeric septin ring, composed of septins, Sep3, Sep4, Sep5 and Sep6 (Dagdas et al., 2012).
235 To test whether exocyst assembly at the pore utilizes the F-actin cytoskeleton or microtubules,
236 we added 10 μ M latrunculin A (an actin depolymerizing agent), 30 μ M benomyl (a microtubule
237 disrupting agent) or 0.1 % DMSO (control) to the conidial suspension after 16 h appressorium
238 development. The exocyst ring was significantly disrupted by latrunculin A treatment ($P < 0.01$,
239 $n = 100$) compared to either benomyl and DMSO (Supplemental Figure 10).

240 The observed physical interaction between the exocyst complex and septin GTPases
241 suggested a role for septins in exocyst organisation (Table 1). Therefore we decided to test
242 whether septins are required for assembly of the exocyst complex at the appressorium pore. To
243 do this, we expressed Sec6-GFP in a Δ *sep3* mutant. During early stages of appressorium
244 formation (4 h) Sec6p showed cortical localization in a Δ *sep3* mutant as in Guy11. During
245 appressorium maturation, however, Sec6p mis-localized in a Δ *sep3* mutant as shown in Figure 5
246 and Supplemental Figure 11). Consistent with this, *M. oryzae* septins are only expressed after 8 h
247 of appressorium development (Dagdas et al., 2012) and we observed transition of the exocyst
248 from the cortex of the appressorium to the pore after 11 h of development. When considered

249 together, these observations suggest that the appressorium pore is first defined by septins and
250 that this is necessary for exocyst organisation (Supplemental Figure 12; Supplemental Movie 6).

251 *CHM1* is a Cla4 homologue of yeast in *M. oryzae*, and a member of the PAK (p21-
252 activated kinase) family that phosphorylates septins. In *M. oryzae*, the $\Delta chm1$ mutant is not able
253 to form either a septin ring or the toroidal F-actin network (Dagdaz et al., 2012). We observed
254 Sec6:GFP in a $\Delta chm1$ mutant and it localized to the cortex of the appressorium at 4 h, but was
255 mislocalized in mature appressoria, failing to organise at the pore (Figure 5A and 5B;
256 Supplemental Figure 11).

257

258 **Exocyst assembly requires regulated synthesis of reactive oxygen species**

259 Septin-mediated plant infection depends on regulated synthesis of reactive oxygen species (ROS)
260 by NADPH oxidases (Ryder et al., 2013). To test whether organization of the exocyst complex is
261 also dependent upon NADPH oxidase activity, we expressed Sec6-GFP in $\Delta noxR$, $\Delta nox1$ and
262 $\Delta nox2$ mutants (Ryder et al., 2013). We found that Sec6-GFP was mis-localized in mature
263 appressoria of $\Delta noxR$ and $\Delta nox2$ mutants (Figure 5A and 5B; Supplemental Figure 11 and 13).
264 However, in a $\Delta nox1$ mutant, Sec6-GFP localised in the same way as in the wild type strain
265 Guy11 (Supplemental Figure 13). This is consistent with the observations made by Ryder et al,
266 (2013) which showed that the NoxR-Nox2 NADPH oxidase is required for septin ring formation
267 at the appressorium pore.

268 In *M. oryzae*, the Pmk1 pathway is regulated through upstream components, including
269 the MAPKKK Mst11, MAPKK Mst7 and an adaptor protein, Mst50 (Park et al., 2006; Wilson &
270 Talbot, 2009; Zhao et al., 2005). The adaptor protein, Mst50, directly interacts with Cdc42 and
271 the Ras2 GTPase suggesting that Pmk1 pathway might be involved the establishment of cell

272 polarity (Park et al., 2006). We therefore decided to investigate Sec6 localisation in a *Δmst12*
273 mutant. *MST12* encodes a transcription factor that acts downstream of the Pmk1 MAP kinase
274 pathway of *M. oryzae* and is required for septin ring formation and plant infection (Dagdaz et al.,
275 2012; Park et al., 2002). Sec6-GFP was completely mis-localised in mature appressoria of a
276 *Δmst12* mutant (Figure 5; Supplemental Figure 11). Consistent with this result, Sec6 and Exo84
277 co-immunoprecipitated both the Mst7 MAPKK and Pmk1 MAPK, suggesting an association
278 with this signalling pathway. We conclude that septin assembly, which requires regulated
279 synthesis of ROS and the action of the Pmk1 MAPK pathway, is necessary for organization and
280 maintenance of the exocyst at the base of the appressorium during plant infection.

281

282 **DISCUSSION**

283 In this study we set out to understand how polarised exocytosis is regulated during appressorium-
284 mediated infection by the rice blast fungus *M. oryzae*. Appressorium infection of rice plants
285 involves generation of cell polarity so that a penetration hypha can form at the base of the
286 infection cell, to rupture the rice cuticle, and invade the underlying rice tissue. Re-polarisation of
287 the appressorium is therefore likely to involve re-modeling of the secretory apparatus to facilitate
288 the morphogenetic changes required for plant infection. Furthermore, fungal pathogens deliver a
289 large repertoire of effector proteins into host plant cells, requiring rapid and focused secretion
290 and very little is currently understood about this process (Kleemann et al., 2012; Giraldo et al.,
291 2013; Irieda et al., 2014). We therefore characterised the exocyst complex of *M. oryzae* and
292 based on the analysis reported here we can make three major conclusions.

293 First of all, we can conclude that the exocyst forms a complex at the tips of growing
294 hyphae, which can be visualised as a crescent-shape at the apex of the tip, in close proximity to,

295 or associated with, the apical plasma membrane. Exocyst proteins are hydrophilic, cytosolic
296 proteins that can associate with membranes (TerBush et al., 2001), consistent with such a
297 location. Our co-immunoprecipitation experiments, meanwhile, confirmed that the exocyst exists
298 as an octameric complex. The exocyst therefore occupies a distinct site from the vesicle supply
299 centre, or Spitzenkörper, which delivers secretory vesicles to the growing tip, consistent with its
300 role in tethering secretory vesicles to the plasma membrane before their SNARE-dependent
301 fusion and cargo deposition (Novick et al., 1981; TerBush et al., 1996). Exocyst localisation in
302 *M. oryzae* is similar to that observed in other filamentous fungi, such as *A. nidulans*, in which the
303 Sec3 homolog SecC is also found in an anterior position to the Spitzenkörper (Taheri-Talesh et
304 al., 2008), and *C. albicans* (Jones and Sudbery, 2010) where the exocyst complex is located in a
305 crescent tip structure. Our findings are distinct, however from exocyst organisation in *N. crassa*
306 where the complex occupies two locations with Sec5, Sec6, Sec8 and Sec15 localizing as a
307 crescent at the hyphal tip, while Exo70 and Exo84 closely associate with the outer layer of the
308 Spitzenkörper (Riquelme et al., 2014). Such differences may be associated with hyphal growth
309 dynamics, since in *Ashbya gossypii*, AgSec3, AgSec5 and AgExo70 localise to the tips of slow-
310 growing hyphae, but to the Spitzenkörper in faster-growing cells (Köhli et al., 2008). Our
311 observation also revealed a highly dynamic and structured tip growth apparatus in *M. oryzae*,
312 with close association of the exocyst with the t-SNARE Sec9 and the Sec4 Rab GTPase, and
313 clear separation from Spitzenkörper-associated proteins such as Mlc1 and the polarisome
314 component Spa2, as well as a clearly defined sub-apical endocytic collar region defined by
315 Fimbrin-GFP localisation.

316 The second major conclusion we can make is that the appressorium pore is the site at
317 which the exocyst assembles prior to plant infection, indicating that polarised exocytosis is

318 required for generation of polarity and protrusion of the penetration peg into plant tissue. At the
319 initial stages of the appressorium development, the *M. oryzae* exocyst shows cortical distribution
320 at the periphery of the appressorium during its radial expansion and turgor generation. Exocyst
321 distribution then changes in a dynamic manner to the base of the appressorium and the distinct
322 appressorium pore from which polar growth is initiated. Analysis of $\Delta exo70$, $\Delta sec5$ and the
323 conditional *Sec6*^{Y601P} mutants all point to the exocyst complex being important for plant
324 infection, highlighting the requirement for polarised exocytosis at this stage of development, not
325 only for penetration peg emergence, but also for the deployment of virulence-associated proteins.
326 The appressorium pore, however, is also a site of endocytosis, as evidenced by the presence of
327 Fimbrin-GFP and BAR domain proteins such as Rvs167 (Dagdas et al., 2012). Recent evidence
328 has suggested that the exocyst may be pivotal to organisation of both endocytosis and exocytosis,
329 acting as a network hub for spatial regulation of these interlinked processes (Jose et al., 2015).
330 Our results are consistent with this idea, since endocytosis and exocytosis both occur within the
331 appressorium pore and must be balanced effectively to ensure plasma membrane homeostasis
332 during rapid polarised extension of the penetration peg.

333 Finally, we can conclude that septins play a key role in recruiting and organising the
334 exocyst to the appressorium pore. It is clear from temporal analysis of exocyst localisation that
335 accumulation at the pore does not occur prior to septin gene expression and ring formation. In
336 *M. oryzae*, septins form a hetero-oligomeric ring around the appressorium pore and Cdc42 is
337 required for ring formation (Dagdas et al., 2012). This is consistent with evidence from budding
338 yeast that deployment of septins to the polarized bud site is also dependent on Cdc42 and that the
339 septin ring is confined by polarized exocytosis to this region (Okada et al., 2013). In yeast,
340 septins compartmentalize the cortex around the cleavage site and maintain both exocyst and

341 polarisome complexes at the bud site by forming a diffusion barrier (Barral et al., 2000;
342 Dobbelaere and Barral, 2004). In *M. oryzae*, septins act as a diffusion barrier at the
343 appressorium, maintaining the position of proteins such as Tea1, a wide range of BAR domain
344 proteins, and the Arp2/3 complex protein, Las17, associated with actin polymerisation,
345 membrane curvature and re-polarisation (Dagdas et al. 2012). This study provides evidence that
346 the exocyst complex is also recruited and spatially organised at the appressorium pore in a
347 septin-dependent manner. Consistent with this idea, the regulated synthesis of ROS, which is
348 required for septin ring formation (Ryder et al., 2013), is also necessary for exocyst recruitment,
349 while the interaction between septins and exocyst components predicted by co-
350 immunoprecipitation is also consistent with their close association.

351 In summary, septin-dependent assembly of the exocyst complex is key to the operation of
352 the specialised infection cell used by the rice blast fungus to gain entry to its host plant. This
353 study is part of an emerging picture of a dynamic infection process that requires integration of
354 diverse signals from the plant to enable a turgor-driven infection process requiring rapid re-
355 polarisation of the appressorium to facilitate cuticle rupture and entry into rice cells. Being able
356 to target the initial stages of plant infection in such a devastating pathogen is likely to be an
357 effective means of ultimately controlling rice blast disease.

358

359

360 **METHODS**

361 **Fungal strains, growth conditions and DNA analysis**

362 All *M. oryzae* isolates used in this study were derived from the wild type strain Guy11 (Leung et
363 al., 1988). Growth conditions and maintenance of *M. oryzae*, fungal transformation, nucleic acid
364 extraction, and appressorium development assays were performed, as previously described
365 (Talbot et al., 1993). Standard procedures were followed for polymerase chain reaction, gel
366 electrophoresis, restriction digestion, DNA gel blots, and DNA sequencing (Sambrook and
367 Russell, 2000).

368 **Plant infection assay**

369 Rice infection assays were carried out using the blast-susceptible cultivar CO-39. Spores were
370 harvested from 10-12 day-old cultures in sterile distilled water and washed twice. A spore
371 suspension was prepared at 5×10^4 spores ml⁻¹ in 0.2% gelatin and sprayed onto 21-day-old rice
372 seedlings using an artist's airbrush. After spray inoculation, plants were kept in plastic bags for
373 48 h to maintain high humidity and then transferred to a plant growth chamber. Plants were
374 incubated for 5-6 days at 24°C with a 12h light-dark cycle and disease symptoms were analyzed
375 (Talbot et al., 1993). All infection assays were repeated three times using 40 seedlings per
376 experiment.

377 **Light and epifluorescence microscopy**

378 Appressorium development assays were performed on hydrophobic borosilicate glass coverslips
379 (Fisher Scientific), as described previously (Ryder et al., 2013). For epifluorescence microscopy,
380 conidia were incubated on coverslips and observed at each time point using an IX-81 inverted
381 microscope (Olympus) and a UPlanSApo X100/1.40 oil objective. Movies were captured using
382 Zeiss LSM510 Meta and Leica SP8 confocal laser scanning microscope systems. Argon (488 nm
383 laser line) and helium-neon (543nm laser line) lasers were used to excite GFP and RFP

384 fluorochromes, respectively, and images recorded under x63 (Zeiss) or x40 (Leica) oil
385 immersion objective lenses. All microscopic images were analyzed using MetaMorph
386 (Molecular Devices), LSM Image browser (Zeiss) or LAS AF (Leica) software. FRAP
387 experiments were carried out using a Leica SP8 confocal microscope, with an Argon (488, nm
388 laser line) to excite GFP for imaging and a 405 nm diode laser to perform photobleaching. Five
389 pre-bleach scans and 100 post-bleach were captured at 1 sec intervals.

390 **Generation of GFP fusion plasmids**

391 All translational GFP-fused constructs were generated by the gap repair cloning method, based
392 on homologous recombination in *S. cerevisiae* (Raymond et al., 1999) using primers shown in
393 Supplemental Table 2. Each fragment was amplified and transformed into a *ura3* strain of *S.*
394 *cerevisiae*. Positive clones were confirmed by colony PCR and used for the plasmid extraction.
395 Schematic diagrams for construction of C- terminal and N-terminal translational fusions is
396 shown in Supplemental Figure S10. In each case, primers contain a 30 bp 5' overlap with
397 adjoining fragments to allow assembly of fragments by homologous recombination. Similarly,
398 the forward primer (Sur.Vec-F) of the sulphonylurea resistance gene cassette (ILV1) (Sweigard
399 et al., 1997), and the reverse primer (TrpC.Vec-R) of the terminator have 30 bp overhangs
400 complementary to the vector sequence (Supplemental Figure 14). N-terminal translational
401 fusions were generated through cloning of the GFP fragment between the native promoter and
402 coding sequence of the corresponding gene (Supplemental Figure 14A). To generate C-terminal
403 translational GFP-fusions, primers were designed to amplify the gene of interest including 2 kb
404 upstream of the start codon, GFP and the TrpC terminator (Supplemental Figure 14B).

405 **Generation of *M. oryzae* *sec6*^{Y601P} temperature-sensitive mutant**

406 A temperature-sensitive *sec6* mutant was generated by point mutation at position Y601P of
407 *SEC6*, based on the previously reported *S. cerevisiae* mutation (L633P) which caused
408 temperature sensitivity (Lamping et al., 2005). In *M. oryzae*, we mutated the same conserved
409 region of Sec6p (Supplemental Figure 5A). The hygromycin resistance cassette (Carroll et al.,
410 1994) was cloned between the coding sequence and terminator of the gene. Restriction sites
411 *Bam*HI and *Hind*III were introduced into Sec6.TS.1F and Sec6.TER.R primers, respectively
412 (Supplemental Table S2). The plasmid was confirmed by DNA sequencing and a *Bam*HI *Hind*III
413 fragment was used for transformation of Guy11. Allelic replacement mutants were selected and
414 checked by colony PCR and Southern blot analysis.

415 ***FM4-64* staining and treatment with chemical inhibitors**

416 FM4-64 solution was prepared as described previously (Bolte et al., 2004). A plug of *M. oryzae*
417 mycelium was inoculated on a water agar slide. After 24h, a 10 μ M aqueous solution of FM4-64
418 was used to stain vegetative hyphae and then incubated for 5 min, before viewing by
419 epifluorescence microscopy. The microtubule-disrupting agent methyl 1-(butylcarbamoyl)-2-
420 benzimidazolecarbamate (benomyl; Fluka) was used at 30 μ M (stock: 10 mM in DMSO) and
421 actin inhibitor latrunculin A (Enzo Life Sciences) was used at 10 μ M (stock: 20 mM in DMSO).
422 Inhibitors were added after 16 h of appressorium development and observations made after 24 h
423 exposure to 0.1 % DMSO was used as the control treatment.

424

425 **Protein secretion Assay**

426 *M. oryzae* mycelium was prepared by growth in liquid CM for 48 h, harvested by filtration
427 through miracloth (Calbiochem) and an equal amount of mycelium transferred to liquid GMM

428 for 24 h. Culture filtrates were collected and subsequently freeze-dried. Lyophilized culture
429 filtrate was re-suspended, diluted and assayed using the Bradford method (Bradford, 1976).
430 Protocol and reagents were obtained from Bio-Rad (Quick Start™ Bradford Kit 2 (500-0207)).

431

432 **Coimmunoprecipitation (Co-IP) Experiments and LC-MS/MS Analysis.**

433 Total protein was extracted from lyophilised *M. oryzae* mycelium after growth in liquid CM for
434 48 h and snap frozen in liquid Nitrogen. *M. oryzae* strains expressing Sec6:GFP, Exo84:GFP and
435 ToxA:GFP (control) were co-immuno-precipitated using the GFP-Trap protocol according to the
436 manufacturer's protocol (ChromoTek). Preparation of peptides for liquid chromatography–
437 tandem mass spectrometry (LC-MS/MS) was performed as follows. Proteins were separated by
438 SDS/PAGE. Gels were cut into slices (~5 Å~ 10 mm) and proteins contained in gel slices
439 prepared for LC-MS/MS, as described previously (Ntoukakis et al., 2009). LC-MS/MS analysis
440 was performed with a LTQ-Orbitrap mass spectrometer (Thermo Scientific) and a nanoflow-
441 HPLC system (nanoACQUITY; Waters Corp.) described previously (Oh et al., 2009) with the
442 following differences: MS/MS peak lists were exported in mascot generic file format by using
443 Discoverer v2.2 (Thermo Scientific). The database was searched with Mascot v2.3 (Matrix
444 Science) with the following differences: (i) The database searched with Mascot v2.3 (Matrix
445 Science) was against *M. oryzae* protein database with the inclusion of sequences of common
446 contaminants such as keratins and trypsin. (ii) Carbamidomethylation of cysteine residues was
447 specified as a fixed modification, and oxidized methionine was allowed as a variable
448 modification. Other Mascot parameters used were as follows: (i) Mass values were mono-
449 isotopic, and the protein mass was unrestricted. (ii) The peptide mass tolerance was 5 ppm, and

450 the fragment mass tolerance was ± 0.6 Da. (iii) Two missed cleavages were allowed with trypsin.
451 All Mascot searches were collated and verified with Scaffold (Proteome Software), and the
452 subset database was searched with X Tandem (The Global Proteome Machine Organization
453 Proteomics Database and Open Source Software; www.thegpm.org). Accepted proteins passed
454 the following threshold in Scaffold: 95% confidence for protein match and minimum of two
455 unique peptide matches with 95 % confidence.

456

457 **Supplemental Material Online**

458 **Supplemental Table 1. List of genes characterised in this study**

459 **Supplemental Table 2. Primers used in this study**

460 **Supplemental Figure 1. Relative transcript abundance of the exocyst subunit-encoding**
461 **genes in mycelium and during appressorium development.**

462 **Supplemental Figure 2. High-resolution epifluorescence micrograph of Sec3-GFP and**
463 **FM4-64-labelled Spitzenkörper in vegetative hyphae of *Magnaporthe oryzae*.**

464 **Supplemental Figure 3. Localisation of Sec2-GFP and FM4-64-labelled Spitzenkörper in**
465 **vegetative hyphae of *Magnaporthe oryzae***

466 **Supplemental Figure 4 Localization of polarized secretory apparatus in growing vegetative**
467 **hyphae.**

468 **Supplemental Figure 5. Exocyst localization during a time course of appressorium**
469 **development in *M. oryzae*.**

470 **Supplemental Figure 6. Localization of polarity determinants in the *M. oryzae***
471 **appressorium.**

472 **Supplemental Figure 7. Quantification of secreted protein from culture filtrates of exocyst**
473 **mutants.**

474 **Supplemental Figure 8. Generation of the *sec6*^{Y601P} temperature-sensitive mutant**

475 **Supplemental Figure 9. Expression and localization of Exo70:GFP, Exo84:GFP,**
476 **Sec15:GFP and Sec3:GFP in the *sec6*^{Y601P} mutant**

477 **Supplemental Figure 10. The F-actin cytoskeleton is required for exocyst ring formation at**
478 **the appressorium pore.**

479 **Supplemental Figure 11. Sec6:GFP localization in $\Delta sep3$, $\Delta noxR$ and $\Delta mst12$ mutants of *M.***
480 ***oryzae*.**

481 **Supplemental Figure 12. Transition of the exocyst from the cortex of the appressorium to**
482 **the appressorial pore during maturation.**

483 **Supplemental Figure 13. Sec6:GFP localization in $\Delta nox1$ and $\Delta nox2$ mutants of *M. oryzae*.**

484 **Supplemental Figure 14. Schematic diagram to show cloning methodology for each GFP**
485 **fusion construct.**

486 **Supplemental Movie 1. Polarisome component Spa2 localizes as a bright spot at the**
487 **growing tip of the hypha.**

488 **Supplemental Movie 2. Fim1:GFP shows cortical actin patches at the sub-apical region of**
489 **the growing hyphae.**

490 **Supplemental Movie 3. GFP-Cdc42 localizes to the tip of the growing hypha.**

491 **Supplemental Movie 4. The v-SNARE Snc1 actively localizes to the tip of the growing**
492 **hypha.**

493 **Supplemental Movie 5. Three-dimensional rotational movie of exocyst sub-unit Sec6**
494 **localized at the base of the appressorium after 24 h.**

495 **Supplemental Movie 6. Transition of the exocyst from the cortex of the appressorium to the**
496 **appressorial pore during maturation.**

497 **during maturation.**

498

499 **Accession Numbers**

500 Accession numbers for *EXO70*, *SEC6*, *SEC10*, *SEC15* are KJ606327, KJ606328, KJ606329 and
501 KJ606330, respectively.

502 **ACKNOWLEDGMENTS**

503 This work was funded by a Halpin Scholarship in Rice Blast Research to YG and a European
504 Research Council, Advanced Investigator Award to NJT under the European Union's Seventh
505 Framework Programme (*FP7/2007-2013*) / ERC grant agreement n° 294702 GENBLAST. We
506 would like to thank Peter Novick and Wei Guo for providing yeast strains. We gratefully
507 acknowledge bioinformatics support of Dr Darren M. Soanes and technical support from Ms.
508 Barbara Saddler.

509 **AUTHOR CONTRIBUTIONS**

510 The research was designed by NJT, YG and YFD. Experiments were executed by YG, YFD, A-
511 LM-R, MJK and GRL. JS and FM carried out mass spectrometry analysis of the exocyst
512 complex. The paper was written by NJT and YG.

513

514 **References**

- 515 Barral, Y., Mermall, V., Mooseker, M.S., and Snyder, M. (2000). Compartmentalization of
516 the cell cortex by septins is required for maintenance of cell polarity in yeast. *Molecular Cell*
517 5, 841-851.
- 518 Bolte, S., Talbot, C., Boutte, Y., Catrice, O., Read, N.D., and Satiat-Jeunemaitre, B. (2004).
519 FM-dyes as experimental probes for dissecting vesicle trafficking in living plant cells. *J*
520 *Microscopy* 214, 159-173.
- 521 Bradford, M.M. (1976). A rapid and sensitive method for the quantitation of microgram
522 quantities of protein utilizing the principle of protein-dye binding. *Analytical Biochemistry*
523 72, 248-254.
- 524 Carroll, A., Sweigard, J., and Valent, B. (1994). Improved vectors for selecting resistance to
525 hygromycin. *Fungal Genet. Newslett.* 41, 22.
- 526 Dagdas, Y.F., Yoshino, K., Dagdas, G., Ryder, L.S., Bielska, E., Steinberg, G., and Talbot,
527 N.J. (2012). Septin-Mediated Plant Cell Invasion by the Rice Blast Fungus, *Magnaporthe*
528 *oryzae*. *Science* 336, 1590-1595.
- 529 de Jong, J.C., McCormack, B.J., Smirnov, N., and Talbot, N.J. (1997). Glycerol generates
530 turgor in rice blast. *Nature* 389, 244-244.

531 Dean, R.A., Talbot, N.J., Ebbole, D.J., Farman, M.L., Mitchell, T.K., Orbach, M.J., Thon,
532 M., Kulkarni, R., Xu, J.R., Pan, H., Read, N.D., Lee, Y.H., Carbone, I., Brown, D., Oh, Y.Y.,
533 Donofrio, N., Jeong, J.S., Soanes, D.M., Djonovic, S., Kolomiets, E., Rehmeier, C., Li, W.,
534 Harding, M., Kim, S., Lebrun, M.H., Bohnert, H., Coughlan, S., Butler, J., Calvo, S., Ma,
535 L.J., Nicol, R., Purcell, S., Nusbaum, C., Galagan, J.E., and Birren, B.W. (2005). The
536 genome sequence of the rice blast fungus *Magnaporthe grisea*. *Nature* 434, 980-986.
537 Dobbelaere, J., and Barral, Y. (2004). Spatial coordination of cytokinetic events by
538 compartmentalization of the cell cortex. *Science* 305, 393-396.
539 Evangelista, M., Zigmond, S., and Boone, C. (2003). Formins: signaling effectors for
540 assembly and polarization of actin filaments. *Journal of Cell Science* 116, 2603-2611.
541 Fischer-Parton, S., Parton, R.M., Hickey, P.C., Dijksterhuis, J., Atkinson, H.A., and Read,
542 N.D. (2000). Confocal microscopy of FM4-64 as a tool for analysing endocytosis and vesicle
543 trafficking in living fungal hyphae. *J Microscopy* 198, 246-259.
544 Giraldo, M.C., and Valent, B. (2013). Filamentous plant pathogen effectors in action. *Nat.*
545 *Rev. Micro.* 11, 800-814.
546 Giraldo, M.C., Dagdas, Y.F., Gupta, Y.K., Mentlak, T.A., Yi, M., Martinez-Rocha, A.L.,
547 Saitoh, H., Terauchi, R., Talbot, N.J., and Valent, B. (2013). Two distinct secretion systems
548 facilitate tissue invasion by the rice blast fungus *Magnaporthe oryzae*. *Nat. Commun.* 4,
549 1996.
550 Guo, W., Grant, A., and Novick, P. (1999). Exo84p is an exocyst protein essential for
551 secretion. *J Biol Chem* 274, 23558-23564.
552 Hall, T. (1999). BioEdit: a user-friendly biological sequence alignment editor and analysis
553 program for Windows 95/98/NT. *Nucl. Acids Symp. Ser.* 41, 95.
554 Hamer, J.E., Howard, R.J., Chumley, F.G., and Valent, B. (1988). A mechanism for surface
555 attachment in spores of a plant pathogenic fungus. *Science* 239, 288-290.
556 He, B., and Guo, W. (2009). The exocyst complex in polarized exocytosis. *Current Opin Cell*
557 *Biol* 21, 537-542.
558 Irieda, H., Maeda, H., Akiyama, K., Hagiwara, A., Saitoh, H., Uemura, A., Terauchi, R., and
559 Takano, Y. (2014). *Colletotrichum orbiculare* Secretes Virulence Effectors to a Biotrophic
560 Interface at the Primary Hyphal Neck via Exocytosis Coupled with SEC22-Mediated Traffic.
561 *The Plant Cell* 26, 2265-2281.
562 Jones, L.A., and Sudbery, P.E. (2010). Spitzenkörper, Exocyst, and Polarisome Components
563 in *Candida albicans* Hyphae Show Different Patterns of Localization and Have Distinct
564 Dynamic Properties. *Eukaryotic Cell* 9, 1455-1465.
565 Jose, M., Tollis, S., Nair, D., Mitteau, R., Velours, C., Massoni-Laporte, A., Royou, A.,
566 Sibarita, J-B., and McCusker, D. (2015). A quantitative imaging-based screen reveals the
567 exocyst as a network hub connecting endo- and exocytosis. *Molec Biol Cell* (online early doi:
568 10.1091/mbc.E14-11-1527).
569 Kershaw, M.J., and Talbot, N.J. (2009). Genome-wide functional analysis reveals that
570 infection-associated fungal autophagy is necessary for rice blast disease. *Proc Natl Acad Sci*
571 *USA* 106, 15967-15972.
572 Khang, C.H., Berruyer, R., Giraldo, M.C., Kankanala, P., Park, S.Y., Czymmek, K., Kang,
573 S., and Valent, B. (2010). Translocation of *Magnaporthe oryzae* effectors into rice cells and
574 their subsequent cell-to-cell movement. *The Plant Cell* 22, 1388-1403.
575 Kleemann, J., Rincon-Rivera, L.J., Takahara, H., Neumann, U., Ver Loren van Themaat, E.,
576 van der Does, H.C., Hacquard, S., Stuber, K., Will, I., Schmalenbach, W., Schmelzer, E. and

577 O'Connell R.J. (2012). Sequential delivery of host-induced virulence effectors by appressoria
578 and intracellular hyphae of the phytopathogen *Colletotrichum higginsianum*. PLoS Pathogens
579 8: e1002643.

580 Köhli, M., Galati, V., Boudier, K., Roberson, R.W., and Philippsen, P. (2008). Growth-
581 speed-correlated localization of exocyst and polarisome components in growth zones of
582 *Ashbya gossypii* hyphal tips. Journal of Cell Science 121, 3878-3889.

583 Lamping, E., Tanabe, K., Niimi, M., Uehara, Y., Monk, B.C., and Cannon, R.D. (2005).
584 Characterization of the *Saccharomyces cerevisiae* sec6-4 mutation and tools to create *S.*
585 *cerevisiae* strains containing the sec6-4 allele. Gene 361, 57-66.

586 Leung, H., Borromeo, S., Bernardo, M.A., and Notteghem, J.L. (1988). Genetic analysis of
587 virulence in the rice blast fungus *Magnaporthe grisea*. Phytopathol. 78, 1227-1233.

588 Novick, P., Ferro, S., and Schekman, R. (1981). Order of events in the yeast secretory
589 pathway. Cell 25, 461-469.

590 Novick, P., Field, C., and Schekman, R. (1980). Identification of 23 complementation groups
591 required for post-translational events in the yeast secretory pathway. Cell 21, 205-215.

592 Novick, P., Medkova, M., Dong, G., Hutagalung, A., Reinisch, K., and Grosshans, B. (2006).
593 Interactions between Rabs, tethers, SNAREs and their regulators in exocytosis. Biochemical
594 Society Transactions 34, 683-686.

595 Ntoukakis, V., Mucyn, T.S., Gimenez-Ibanez, S., Chapman, H.C., Gutierrez, J.R., Balmuth,
596 A.L., Jones, A.M.E., and Rathjen, J.P. (2009). Host Inhibition of a Bacterial Virulence
597 Effector Triggers Immunity to Infection. Science 324, 784-787.

598 Oh, S.-K., Young, C., Lee, M., Oliva, R., Bozkurt, T.O., Cano, L.M., Win, J., Bos, J.I.B.,
599 Liu, H.-Y., van Damme, M., Morgan, W., Choi, D., Van der Vossen, E.A.G., Vleeshouwers,
600 V.G.A.A., and Kamoun, S. (2009). In Planta Expression Screens of *Phytophthora infestans*
601 RXLR Effectors Reveal Diverse Phenotypes, Including Activation of the *Solanum*
602 *bulbocastanum* Disease Resistance Protein Rpi-blb2. The Plant Cell 21, 2928-2947.

603 Okada, S., Leda, M., Hanna, J., Savage, N.S., Bi, E., and Goryachev, A.B. (2013). Daughter
604 cell identity emerges from the interplay of Cdc42, septins, and exocytosis. Developmental
605 Cell 26, 148-161.

606 Park, G., Xue, C., Zhao, X., Kim, Y., Orbach, M. and Xu, J.R. (2006). Multiple upstream
607 signals converge on the adaptor protein Mst50 in *Magnaporthe grisea*. The Plant Cell 18,
608 2822-2835.

609 Park, G., Xue, C., Zheng, L., Lam, S., and Xu, J.R. (2002). MST12 regulates infectious
610 growth but not appressorium formation in the rice blast fungus *Magnaporthe grisea*. Molec
611 Plant Microbe Interact 15, 183-192.

612 Raymond, C.K., Pownder, T.A., and Sexson, S.L. (1999). General method for plasmid
613 construction using homologous recombination. BioTechniques 26, 134-138, 140-131.

614 Read, N.D. (2011). Exocytosis and growth do not occur only at hyphal tips. Mol Microbiol
615 81, 4-7.

616 Riquelme, M. (2013). Tip growth in filamentous fungi: a road trip to the apex. Annu. Rev.
617 Microbiol. 67, 587-609.

618 Riquelme, M., Bartnicki-García, S., González-Prieto, J.M., Sánchez-León, E., Verdín-
619 Ramos, J.A., Beltrán-Aguilar, A., and Freitag, M. (2007). Spitzenkörper Localization and
620 Intracellular Traffic of Green Fluorescent Protein-Labeled CHS-3 and CHS-6 Chitin
621 Synthases in Living Hyphae of *Neurospora crassa*. Eukaryotic Cell 6, 1853-1864.

622 Riquelme, M., Bredeweg, E.L., Callejas-Negrete, O., Roberson, R.W., Ludwig, S., Beltran-
623 Aguilar, A., Seiler, S., Novick, P., and Freitag, M. (2014). The *Neurospora crassa* exocyst
624 complex tethers Spitzenkorper vesicles to the apical plasma membrane during polarized
625 growth. *Mol Biol Cell* 25, 1312-1326.

626 Ryder, L.S., Dagdas, Y.F., Mentlak, T.A., Kershaw, M.J., Thornton, C.R., Schuster, M.,
627 Chen, J., Wang, Z., and Talbot, N.J. (2013). NADPH oxidases regulate septin-mediated
628 cytoskeletal remodeling during plant infection by the rice blast fungus. *Proc Natl Acad Sci*
629 *USA* 110, 3179-3184.

630 Sagot, I., Klee, S.K., and Pellman, D. (2002). Yeast formins regulate cell polarity by
631 controlling the assembly of actin cables. *Nature Cell Biol* 4, 42-50.

632 Salminen, A., and Novick, P.J. (1989). The Sec15 protein responds to the function of the
633 GTP binding protein, Sec4, to control vesicular traffic in yeast. *J Cell Biol* 109, 1023-1036.

634 Sambrook, J., and Russell, D.W. (2000). *Molecular cloning : A Laboratory Manual*. 3rd ed.
635 (Cold Spring Harbour Laboratory Press, New York, USA).

636 Saunders, D.G.O., Aves, S.J., and Talbot, N.J. (2010). Cell Cycle–Mediated Regulation of
637 Plant Infection by the Rice Blast Fungus. *The Plant Cell* 22, 497-507.

638 Sheu, Y.J., Santos, B., Fortin, N., Costigan, C., and Snyder, M. (1998). Spa2p interacts with
639 cell polarity proteins and signaling components involved in yeast cell morphogenesis. *Molec*
640 *Cell Biol* 18, 4053-4069.

641 Soanes, D.M., Chakrabarti, A., Paszkiewicz, K.H., Dawe, A.L., and Talbot, N.J. (2012).
642 Genome-wide Transcriptional Profiling of Appressorium Development by the Rice Blast
643 Fungus *Magnaporthe oryzae*. *PLoS Pathog* 8(2): e1002514.

644 Songer, J.A., and Munson, M. (2009). Sec6p anchors the assembled exocyst complex at sites
645 of secretion. *Mol. Biol. Cell.* 20, 973-982.

646 Stalder, D., Mizuno-Yamasaki, E., Ghassemian, M., and Novick, P.J. (2013).
647 Phosphorylation of the Rab exchange factor Sec2p directs a switch in regulatory binding
648 partners. *Proceedings of the National Academy of Sciences* 110, 19995-20002.

649 Steinberg, G. (2007). Hyphal Growth: a Tale of Motors, Lipids, and the Spitzenkörper.
650 *Eukaryotic Cell* 6, 351-360.

651 Sudbery, P. (2011a). Fluorescent proteins illuminate the structure and function of the hyphal
652 tip apparatus. *Fungal Genet Biol* 48, 849-857.

653 Sudbery, P.E. (2011b). Growth of *Candida albicans* hyphae. *Nat. Rev. Micro.* 9, 737-748.

654 Sweigard, J., Chumly, F., Carrol, A., Farrall, L., and Valent, B. (1997). A series of vectors
655 for fungal transformation. *Fungal Genet. Newsl.*, 52-55.

656 Taheri-Talesh, N., Horio, T., Araujo-Bazan, L., Dou, X., Espeso, E.A., Penalva, M.A.,
657 Osmani, S.A., and Oakley, B.R. (2008). The tip growth apparatus of *Aspergillus nidulans*.
658 *Mol Biol Cell* 19, 1439-1449.

659 Talbot, N.J., Ebbole, D.J., and Hamer, J.E. (1993). Identification and characterization of
660 MPG1, a gene involved in pathogenicity from the rice blast fungus *Magnaporthe grisea*. *The*
661 *Plant Cell* 5, 1575-1590.

662 TerBush, D.R., Guo, W., Dunkelbarger, S., and Novick, P. (2001). Purification and
663 characterization of yeast exocyst complex. *Methods in Enzymology* 329, 100-110.

664 TerBush, D.R., Maurice, T., Roth, D., and Novick, P. (1996). The Exocyst is a multiprotein
665 complex required for exocytosis in *Saccharomyces cerevisiae*. *EMBO J* 15, 6483-6494.

666 Thompson, J.D., Higgins, D.G., and Gibson, T.J. (1994). CLUSTAL W: improving the
667 sensitivity of progressive multiple sequence alignment through sequence weighting, position-
668 specific gap penalties and weight matrix choice. *Nucleic Acids Res.* 22, 4673-4680.
669 Veneault-Fourrey, C., Barooah, M., Egan, M., Wakley, G., and Talbot, N.J. (2006).
670 Autophagic Fungal Cell Death Is Necessary for Infection by the Rice Blast Fungus. *Science*
671 312, 580-583.
672 Verdin, J., Bartnicki-Garcia, S., and Riquelme, M. (2009). Functional stratification of the
673 Spitzenkorper of *Neurospora crassa*. *Mol Microbiol* 74, 1044-1053.
674 Wiederkehr, A., Du, Y., Pypaert, M., Ferro-Novick, S., and Novick, P. (2003). Sec3p is
675 needed for the spatial regulation of secretion and for the inheritance of the cortical
676 endoplasmic reticulum. *Mol Biol Cell* 14, 4770-4782.
677 Wilson, R.A., and Talbot, N.J. (2009). Under pressure: investigating the biology of plant
678 infection by *Magnaporthe oryzae*. *Nature Rev Microbiol* 7, 185-195.
679 Xu, J.R., and Hamer, J.E. (1996). MAP kinase and cAMP signaling regulate infection
680 structure formation and pathogenic growth in the rice blast fungus *Magnaporthe grisea*.
681 *Genes Dev* 10, 2696-2706.
682 Zhao, X., Kim, Y., Park, G. and Xu, J.R. (2005). A mitogen-activated protein kinase cascade
683 regulating infection-related morphogenesis in *Magnaporthe grisea*. *The Plant Cell* 17, 1317-
684 1329.
685
686

687 **Table 1. Putative exocyst-interacting proteins in *M. oryzae* identified by co-**
688 **immunoprecipitation of *SEC6* and *EXO84***

<i>M. oryzae</i> proteins identified by Co-IP		Total Spectral Count/ Total protein coverage (%)		
		Sec6:GFP	Exo84:GFP	Control
Exocyst	Sec3 (MGG_03323)	164/35	69/25	0/0
	Sec5 (MGG_07150)	35/29	57/48	0/0
	Sec6 (MGG_03235)	100/55	27/34	0/0
	Sec8 (MGG_03985)	153/61	48/42	0/0
	Sec10 (MGG_04559)	9/13	119/64	0/0
	Sec15 (MGG_00471)	7/11	77/54	0/0
	Exo70 (MGG_01760)	11/14	163/83	0/0
	Exo84 (MGG_06098)	10/13	191/86	0/0
Septins	Sep6 (MGG_07466)	2/12	1/2	0/0
	Sep4 (MGG_06726)	0/0	10/27	0/0
	Sep3 (MGG_01521)	2/3	0/0	0/0
	Sep5 (MGG_03087)	0/0	2/5	0/0
Actin binding	Fim1 (MGG_04478)	2/5	3/5	0/0
	Vps1/Dynamain (MGG_09517)	2/3	0/0	1/1
Rho-GTPase	Rho1 (MGG_07176)	8/22	2/16	0/0
	Rac1 (MGG_02731)	3/19	0/0	0/0
MAPK signalling pathway	Mst7 (MGG_06482)	6/3	8/3	1/0
	Pmk1 (MGG_09565)	2/5	6/19	0/0
	Mps1 (MGG_04943)	3/10	0/0	0/0
Others	Sec14 (MGG_00905)	2/17	4/12	0/0
	Sec26 (MGG_06860)	4/6	1/1	1/0
	Ypt1 (MGG_06962)	6/37	1/6	0/0
	Sec24 (MGG_09564)	3/3	1/1	0/0
	Sec63 (MGG_05320)	2/2	0/0	0/0
	Arb1(ABC transporter) (MGG_11862)	5/5	2/1	0/0
	Hex1 (Woronin body protein) (MGG_02696)	9/75	2/5	0/0

689

690 **Figure legends**

691 **Figure 1. Localisation of the exocyst complex in vegetative hyphae of *M. oryzae*.**

692 Micrographs and corresponding linescan graphs to show localisation of the exocyst complex and
693 the Spitzenkörper in growing hyphae of *M. oryzae*. Strains of the fungus expressing Sec8-GFP,
694 Exo70-GFP, Exo84-GFP, Sec5-GFP, Sec6-GFP, Sec3-GFP and Sec15-GFP were prepared with
695 each gene fusion expressed under control of its native promoter. Each strain was incubated
696 overnight at 24°C on a 0.8% distilled water agar slide in a humid chamber. The lipophilic dye,
697 FM4-64, was then used to label the Spitzenkörper. Epifluorescence micrographs were overlaid to
698 observe relative localisation and a line scan graph generated. Scale bar=10µm.

699 **Figure 2. Expression of *M. oryzae* exocyst sub-units during appressorium development.**

700 **(A)** *M. oryzae* Sec6 expressed with c-terminal GFP fusion under native promoter. During initial
701 stages of conidial germination and germ tube formation Sec6 localized to the germ tube tip and
702 during early stages of appressorium formation Sec6-GFP localized to the periphery of the
703 appressorium at the plasma-membrane. After 24 h, Sec6 expressed at the base of the
704 appressorium and formed ring at the appressorial pore.

705 **(B)** Micrograph of the other exocyst subunits Exo70, Sec5, Exo84, Sec8, Sec3 and Sec15 formed
706 ring at the appressorium pore after 24 h. Linescan graphs show each exocyst-GFP fluorescence
707 in the appressorium.

708 (C) Colocalization Sec6-GFP and LifeAct-RFP in the mature appressoria and linescan graph
709 consistent with colocalization of the exocyst ring and actin network around the appressoria pore.
710 Scale bar=10 μ m.

711 **Figure 3. Exocyst sub-units are required for secretion of spore tip mucilage during plant**
712 **infection.**

713 (A) Mucilage secreted from the conidia stained with FITC-ConA. The conidial suspension of $5 \times$
714 10^4 ml⁻¹ from wild type Guy11, Δ *exo70* and Δ *sec5* mutant strains were inoculated onto glass
715 coverslips. Conidia from all the strains were used to stain with FITC-ConA after 1/2 h and 24 h of
716 inoculation. Scale bar = 10 μ m.

717 (B) Bar chart showing percentage of conidia/ appressorium strongly labelled with FITC-ConA
718 after 1/2 h (black bars) and 24 h (grey bars). Values are mean \pm S.D. for three repetitions of the
719 experiment, n = 300.

720 (C) Bar chart showing number of lesions per 5 cm on susceptible rice cultivar Co-39 sprayed
721 with Guy11, Δ *exo70* and Δ *sec5* mutant strains (P<0.05 for all mutants, n = 30 for each strain,
722 mean \pm S.D., three experiments).

723 (D) Conidial suspension of 5×10^4 ml⁻¹ from Guy11, Δ *exo70* and Δ *sec5* mutant were sprayed on
724 3 weeks old seedlings of susceptible rice cultivar Co-39. Disease symptoms were quantified after
725 5 d of incubation in growth chamber.

726 **Figure 4. Sec6 is necessary for exocyst assembly at the appressorium pore.**

727 (A) Temperature sensitivity of the *sec6*^{Y601P} mutant was tested by the comparison of the hyphal
728 growth of ectopic transformant (*sec6-2*) and wild type Guy11 after incubation at the semi-
729 restrictive temperature of 29 °C for 4 d and restoration of hyphal growth was done by incubation
730 for a further 3 d at 24 °C.

731 (B) Micrograph showing localization of exocyst subunits Sec5:GFP and Sec8:GFP in
732 temperature sensitive mutant *sec6*^{Y601P} at permissive temperature 24 °C and semi restrictive
733 temperature 29 °C. Exocyst ring was completely mislocalized at semi restrictive temperature 29
734 °C in *sec6*^{Y601P} mutant. Scale bar = 10 µm.

735 (C) Bar chart showing percentage of appressorium expressing exocyst subunit Sec5:GFP and
736 Sec8:GFP at permissive temperature 24 °C (black bars) and semi restrictive temperature 29 °C
737 (grey bars). Values are mean ± S.D. for three repetitions of the experiment, n = 300.

738 (D) Bar chart showing number of lesions per 5 cm on susceptible rice cultivar Co-39 sprayed
739 with the wild type Guy11 and temperature sensitive mutant *sec6*^{Y601P} strains at permissive
740 temperature 24 °C (black bars) and semi restrictive temperature 29 °C (grey bars) (P<0.05 for all
741 mutants, n = 30 for each strain, mean ± S.D., three experiments).

742 (E) *sec6*^{Y601P} mutant and *guy11* were sprayed on susceptible rice cultivar Co-39 with the conidial
743 concentration of 5×10^4 ml⁻¹ and incubated for 5 days at permissive temperature 24 °C and semi
744 restrictive temperature 29 °C.

745 **Figure 5. Recruitment of the exocyst complex to the appressorium pore is septin-**
746 **dependent.**

747 **(A)** Micrographs of exocyst sub-unit Sec6:GFP expressed in wild type strain Guy11, $\Delta sep3$,
748 $\Delta chm1$, $\Delta noxR$ and $\Delta mst12$, mutants. Conidial suspensions at $5 \times 10^4 \text{ ml}^{-1}$ were inoculated onto
749 glass coverslips and the expression of Sec6:GFP was checked at 4 h and 24 h after inoculation.
750 Scale bar = 10 μm .

751 **(B)** Bar chart showing percentage of appressorium expressing exocyst subunit Sec6:GFP at 4 h
752 (black bars) and 24 h (grey bars) after inoculation. Values are mean \pm S.D. for three repetitions
753 of the experiment, n = 300.

754

755

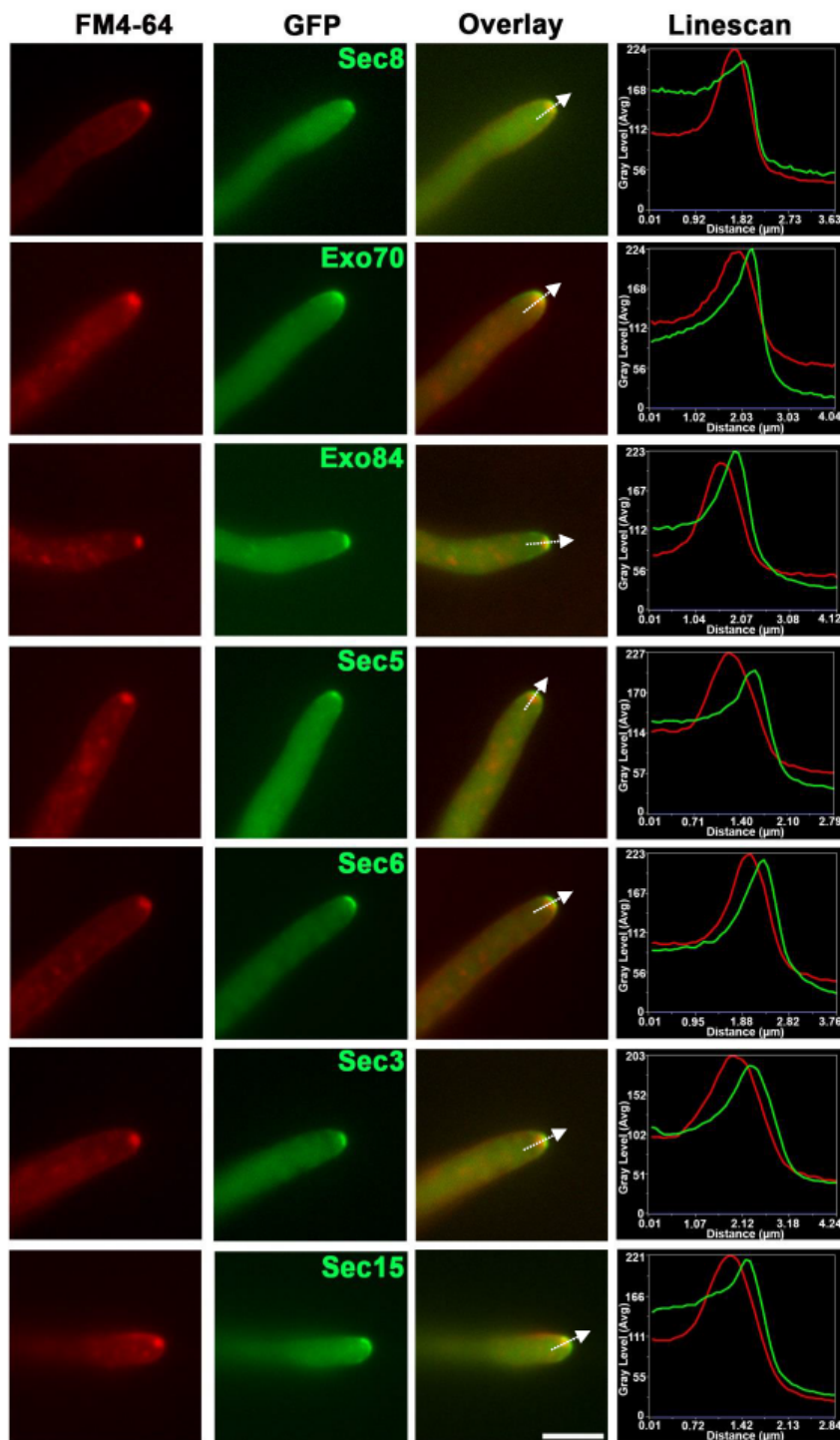


Figure1. Localisation of the exocyst complex in vegetative hyphae of *M. oryzae*. Micrographs and corresponding linescan graphs to show localisation of the exocyst complex and the Spitzenkörper in growing hyphae of *M. oryzae*. Strains of the fungus expressing Sec8-GFP, Exo70-GFP, Exo84-GFP, Sec5-GFP, Sec6-GFP, Sec3-GFP and Sec15-GFP were prepared with each gene fusion expressed under control of its native promoter. Each strain was incubated overnight at 24°C on a 0.8% distilled water agar slide in a humid chamber. The lipophilic dye, FM4-64, was then used to label the Spitzenkörper. Epifluorescence micrographs were overlaid to observe relative localisation and a line scan graph generated. Scale bar=10µm.

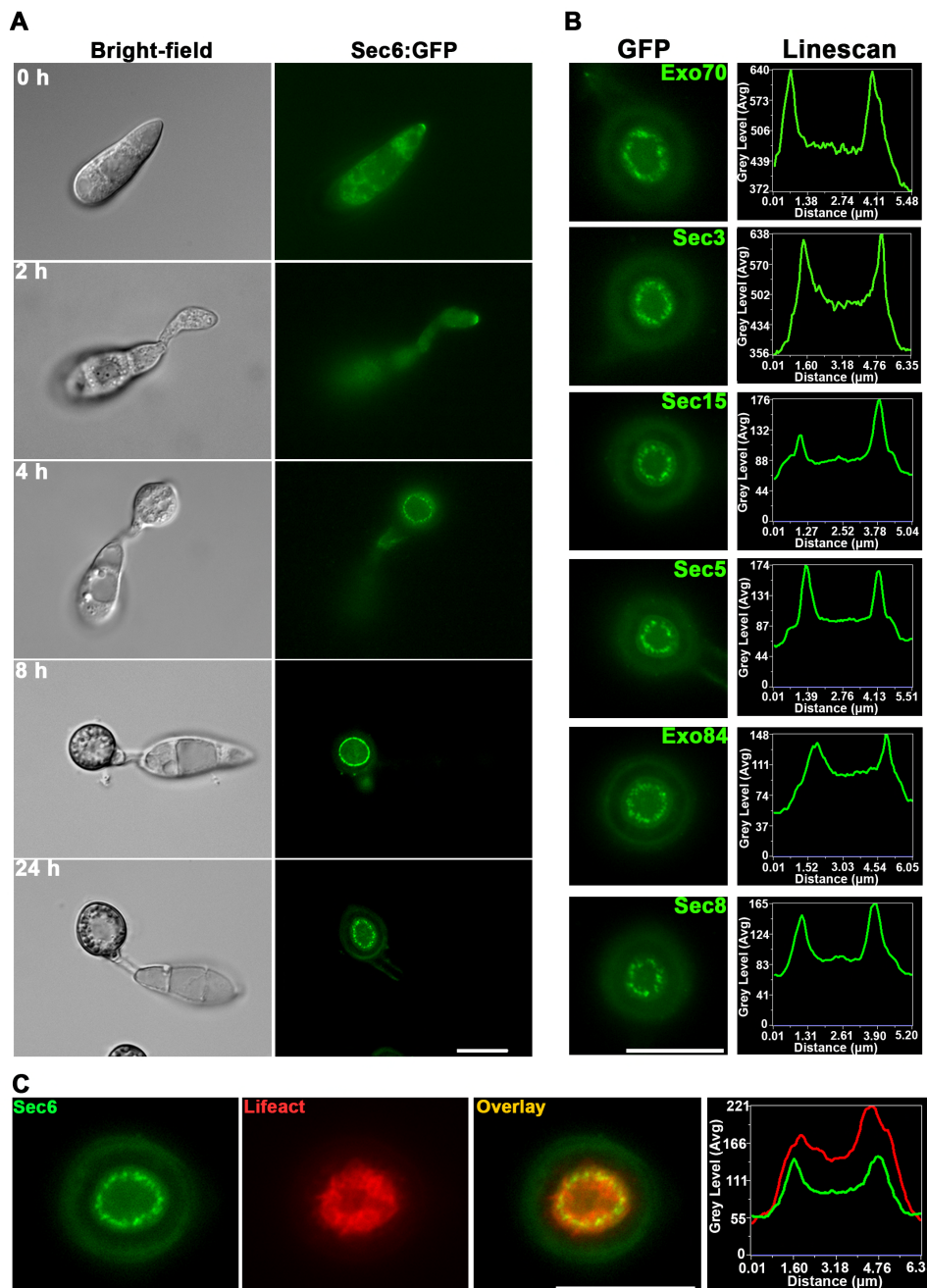


Figure 2. Expression of *M. oryzae* exocyst sub-units during appressorium development.

(A) *M. oryzae* Sec6 expressed with c-terminal GFP fusion under native promoter. During initial stages of conidial germination and germ tube formation Sec6 localized to the germ tube tip and during early stages of appressorium formation Sec6-GFP localized to the periphery of the appressorium at the plasma-membrane. After 24 h, Sec6 expressed at the base of the appressorium and formed ring at the appressorial pore.

(B) Micrograph of the other exocyst subunits Exo70, Sec5, Exo84, Sec8, Sec3 and Sec15 formed ring at the appressorium pore after 24 h. Linescan graphs show each exocyst-GFP fluorescence in the appressorium.

(C) Colocalization Sec6-GFP and LifeAct-RFP in the mature appressoria and linescan graph consistent with colocalization of the exocyst ring and actin network around the appressoria pore. Scale bar=10 μ m.

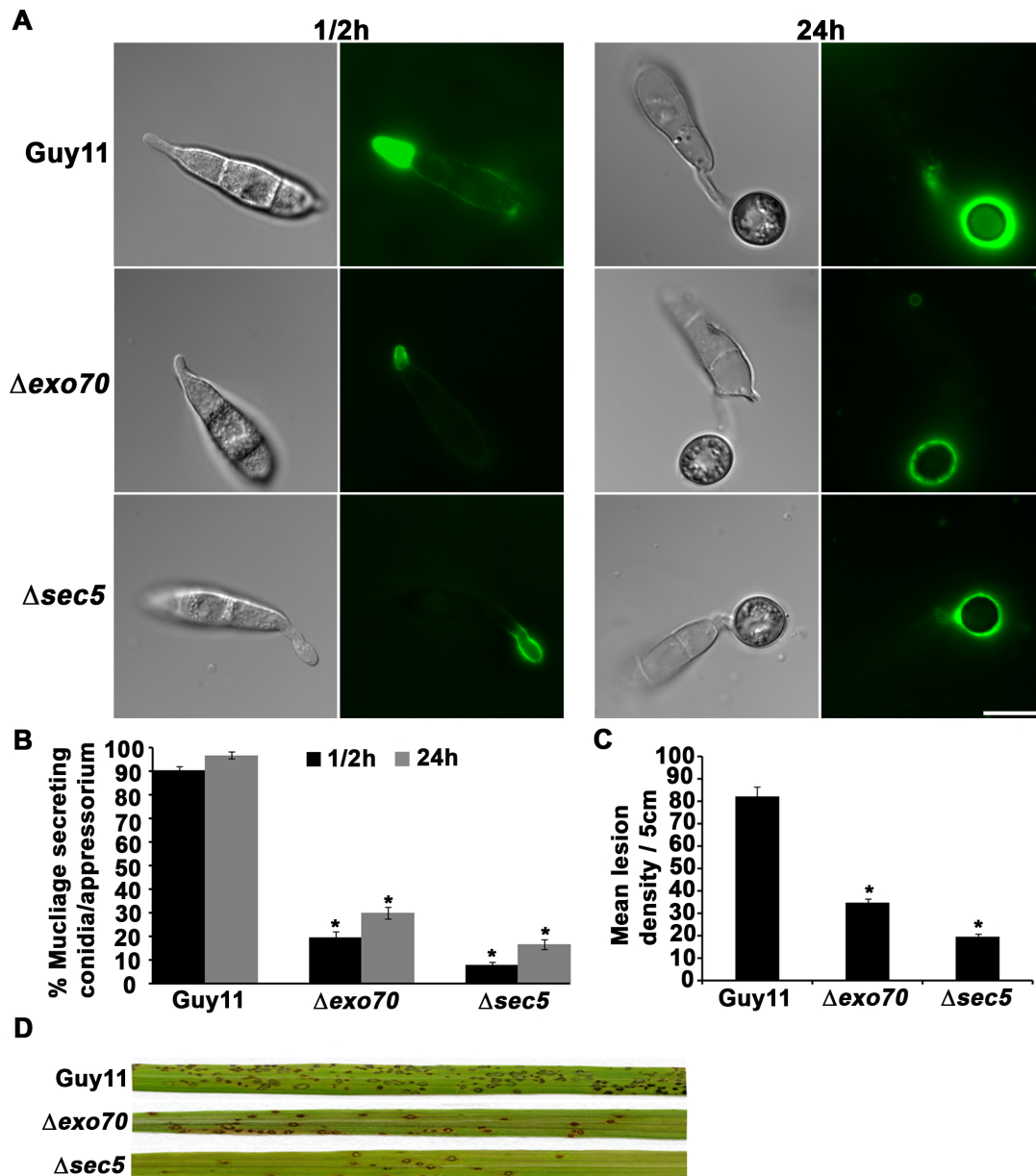


Figure 3. Exocyst sub-units are required for secretion of spore tip mucilage during plant infection.

(A) Mucilage secreted from the conidia stained with FITC-ConA. The conidial suspension of $5 \times 10^4 \text{ ml}^{-1}$ from wild type Guy11, Δ exo70 and Δ sec5 mutant strains were inoculated onto glass coverslips. Conidia from all the strains were used to stain with FITC-ConA after 1/2 h and 24 h of inoculation. Scale bar = 10 μm .

(B) Bar chart showing percentage of conidia/ appressorium strongly labelled with FITC-ConA after 1/2 h (black bars) and 24 h (grey bars). Values are mean \pm S.D. for three repetitions of the experiment, $n = 300$.

(C) Bar chart showing number of lesions per 5 cm on susceptible rice cultivar Co-39 sprayed with Guy11, Δ exo70 and Δ sec5 mutant strains ($P < 0.05$ for all mutants, $n = 30$ for each strain, mean \pm S.D., three experiments).

(D) Conidial suspension of $5 \times 10^4 \text{ ml}^{-1}$ from Guy11, Δ exo70 and Δ sec5 mutant were sprayed on 3 weeks old seedlings of susceptible rice cultivar Co-39. Disease symptoms were quantified after 5 d of incubation in growth chamber.

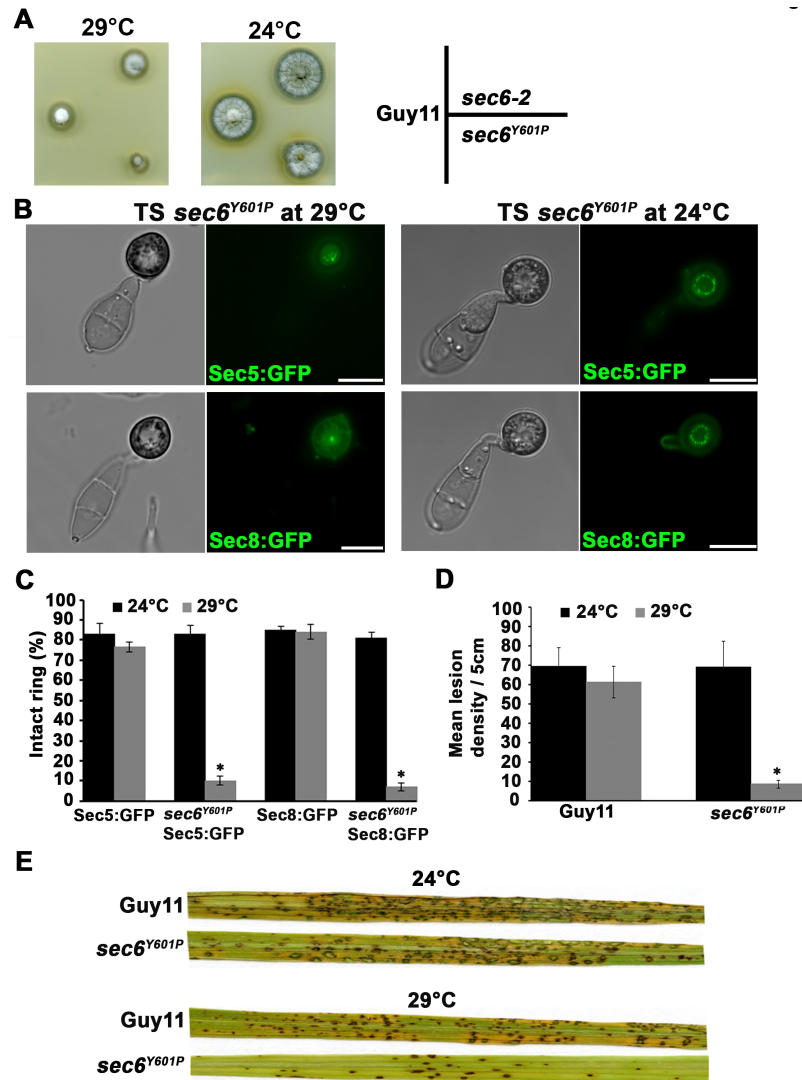


Figure 4. Sec6 is necessary for exocyst assembly at the appressorium pore.

(A) Temperature sensitivity of the *sec6^{Y601P}* mutant was tested by the comparison of the hyphal growth of ectopic transformant (*sec6-2*) and wild type Guy11 after incubation at the semi-restrictive temperature of 29 °C for 4 d and restoration of hyphal growth was done by incubation for a further 3 d at 24 °C.

(B) Micrograph showing localization of exocyst subunits Sec5:GFP and Sec8:GFP in temperature sensitive mutant *sec6^{Y601P}* at permissive temperature 24 °C and semi restrictive temperature 29 °C. Exocyst ring was completely mislocalized at semi restrictive temperature 29 °C in *sec6^{Y601P}* mutant. Scale bar = 10 μm.

(C) Bar chart showing percentage of appressorium expressing exocyst subunit Sec5:GFP and Sec8:GFP at permissive temperature 24 °C (black bars) and semi restrictive temperature 29 °C (grey bars). Values are mean ± S.D. for three repetitions of the experiment, n = 300.

(D) Bar chart showing number of lesions per 5 cm on susceptible rice cultivar Co-39 sprayed with the wild type Guy11 and temperature sensitive mutant *sec6^{Y601P}* strains at permissive temperature 24 °C (black bars) and semi restrictive temperature 29 °C (grey bars) (P<0.05 for all mutants, n = 30 for each strain, mean ± S.D., three experiments).

(E) *sec6^{Y601P}* mutant and guy11 were sprayed on susceptible rice cultivar Co-39 with the conidial concentration of 5×10^4 ml⁻¹ and incubated for 5 days at permissive temperature 24 °C and semi restrictive temperature 29 °C.

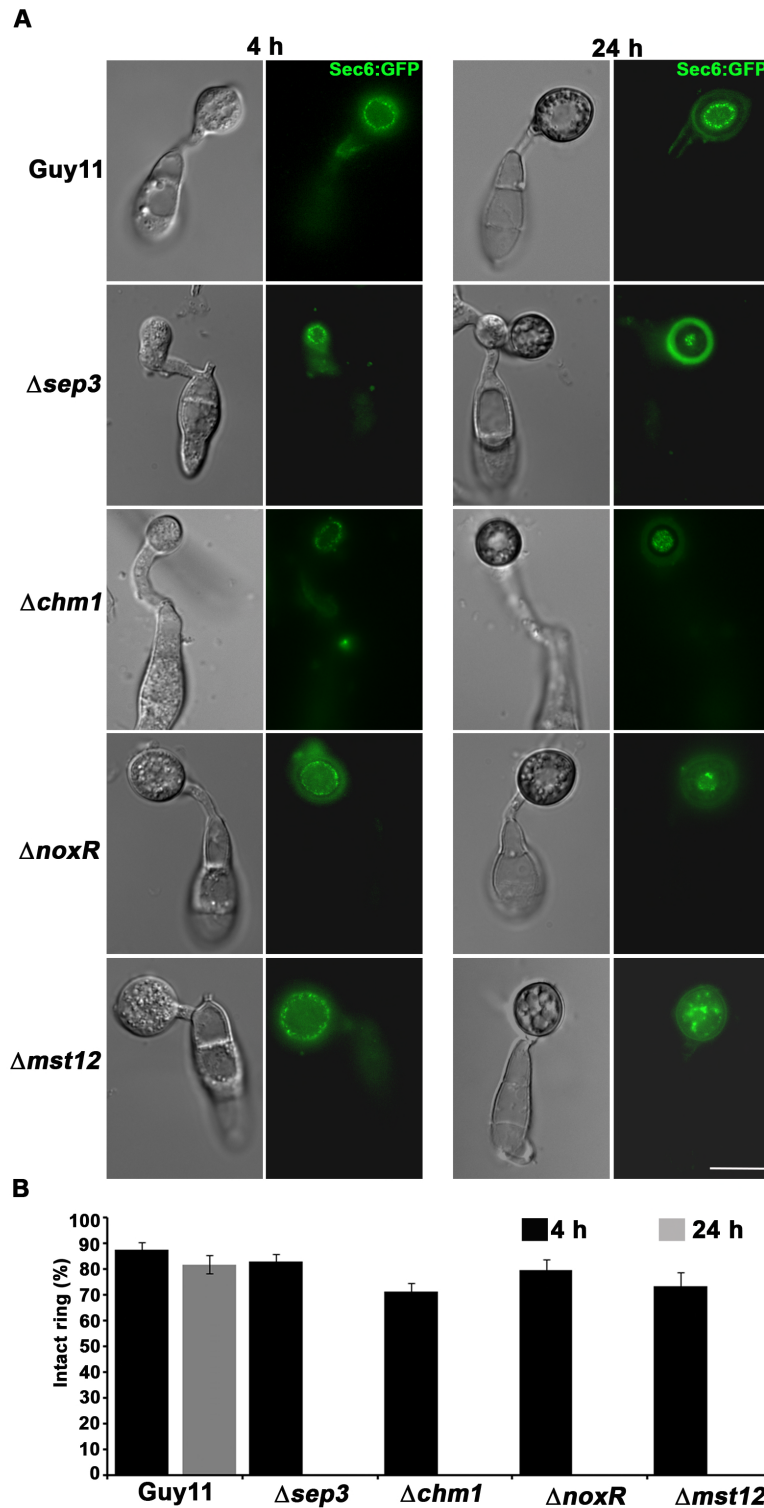


Figure 5. Recruitment of the exocyst complex to the appressorium pore is septin-dependent.

(A) Micrographs of exocyst sub-unit Sec6:GFP expressed in wild type strain Guy11, $\Delta sep3$, $\Delta chm1$, $\Delta noxR$ and $\Delta mst12$, mutants. Conidial suspensions at $5 \times 10^4 \text{ ml}^{-1}$ were inoculated onto glass coverslips and the expression of Sec6:GFP was checked at 4 h and 24 h after inoculation. Scale bar = 10 μm .

(B) Bar chart showing percentage of appressorium expressing exocyst subunit Sec6:GFP at 4 h (black bars) and 24 h (grey bars) after inoculation. Values are mean \pm S.D. for three repetitions of the experiment, $n = 300$.

Table 1. Putative exocyst-interacting proteins in *M. oryzae* identified by co-immunoprecipitation of *SEC6* and *EXO84*

<i>M. oryzae</i> proteins identified by Co-IP		Total Spectral Count/ Total protein coverage (%)		
		Sec6:GFP	Exo84:GFP	Control
Exocyst	Sec3 (MGG_03323)	164/35	69/25	0/0
	Sec5 (MGG_07150)	35/29	57/48	0/0
	Sec6 (MGG_03235)	100/55	27/34	0/0
	Sec8 (MGG_03985)	153/61	48/42	0/0
	Sec10 (MGG_04559)	9/13	119/64	0/0
	Sec15 (MGG_00471)	7/11	77/54	0/0
	Exo70 (MGG_01760)	11/14	163/83	0/0
	Exo84 (MGG_06098)	10/13	191/86	0/0
Septins	Sep6 (MGG_07466)	2/12	1/2	0/0
	Sep4 (MGG_06726)	0/0	10/27	0/0
	Sep3 (MGG_01521)	2/3	0/0	0/0
	Sep5 (MGG_03087)	0/0	2/5	0/0
Actin binding	Fim1 (MGG_04478)	2/5	3/5	0/0
	Vps1/Dynamain (MGG_09517)	2/3	0/0	1/1
Rho-GTPase	Rho1 (MGG_07176)	8/22	2/16	0/0
	Rac1 (MGG_02731)	3/19	0/0	0/0
MAPK signalling pathway	Mst7 (MGG_06482)	6/3	8/3	1/0
	Pmk1 (MGG_09565)	2/5	6/19	0/0
	Mps1 (MGG_04943)	3/10	0/0	0/0
Others	Sec14 (MGG_00905)	2/17	4/12	0/0
	Sec26 (MGG_06860)	4/6	1/1	1/0
	Ypt1 (MGG_06962)	6/37	1/6	0/0
	Sec24 (MGG_09564)	3/3	1/1	0/0
	Sec63 (MGG_05320)	2/2	0/0	0/0
	Arb1(ABC transporter) (MGG_11862)	5/5	2/1	0/0
	Hex1 (Woronin body protein) (MGG_02696)	9/75	2/5	0/0

Parsed Citations

Barral, Y., Mermall, V., Mooseker, M.S., and Snyder, M. (2000). Compartmentalization of the cell cortex by septins is required for maintenance of cell polarity in yeast. *Molecular Cell* 5, 841-851.

Pubmed: [Author and Title](#)

CrossRef: [Author and Title](#)

Google Scholar: [Author Only](#) [Title Only](#) [Author and Title](#)

Bolte, S., Talbot, C., Boutte, Y., Catrice, O., Read, N.D., and Satiat-Jeunemaitre, B. (2004). FM-dyes as experimental probes for dissecting vesicle trafficking in living plant cells. *J Microscopy* 214, 159-173.

Pubmed: [Author and Title](#)

CrossRef: [Author and Title](#)

Google Scholar: [Author Only](#) [Title Only](#) [Author and Title](#)

Bradford, M.M. (1976). A rapid and sensitive method for the quantitation of microgram quantities of protein utilizing the principle of protein-dye binding. *Analytical Biochemistry* 72, 248-254.

Pubmed: [Author and Title](#)

CrossRef: [Author and Title](#)

Google Scholar: [Author Only](#) [Title Only](#) [Author and Title](#)

Carroll, A., Sweigard, J., and Valent, B. (1994). Improved vectors for selecting resistance to hygromycin. *Fungal Genet. Newslett.* 41, 22.

Pubmed: [Author and Title](#)

CrossRef: [Author and Title](#)

Google Scholar: [Author Only](#) [Title Only](#) [Author and Title](#)

Dagdas, Y.F., Yoshino, K., Dagdas, G., Ryder, L.S., Bielska, E., Steinberg, G., and Talbot, N.J. (2012). Septin-Mediated Plant Cell Invasion by the Rice Blast Fungus, *Magnaporthe oryzae*. *Science* 336, 1590-1595.

Pubmed: [Author and Title](#)

CrossRef: [Author and Title](#)

Google Scholar: [Author Only](#) [Title Only](#) [Author and Title](#)

de Jong, J.C., McCormack, B.J., Smirnov, N., and Talbot, N.J. (1997). Glycerol generates turgor in rice blast. *Nature* 389, 244-244.

Pubmed: [Author and Title](#)

CrossRef: [Author and Title](#)

Google Scholar: [Author Only](#) [Title Only](#) [Author and Title](#)

Dean, R.A., Talbot, N.J., Ebbole, D.J., Farman, M.L., Mitchell, T.K., Orbach, M.J., Thon, M., Kulkarni, R., Xu, J.R., Pan, H., Read, N.D., Lee, Y.H., Carbone, I., Brown, D., Oh, Y.Y., Donofrio, N., Jeong, J.S., Soanes, D.M., Djonovic, S., Kolomiets, E., Rehmeier, C., Li, W., Harding, M., Kim, S., Lebrun, M.H., Bohnert, H., Coughlan, S., Butler, J., Calvo, S., Ma, L.J., Nicol, R., Purcell, S., Nusbaum, C., Galagan, J.E., and Birren, B.W. (2005). The genome sequence of the rice blast fungus *Magnaporthe grisea*. *Nature* 434, 980-986.

Pubmed: [Author and Title](#)

CrossRef: [Author and Title](#)

Google Scholar: [Author Only](#) [Title Only](#) [Author and Title](#)

Dobbelaere, J., and Barral, Y. (2004). Spatial coordination of cytokinetic events by compartmentalization of the cell cortex. *Science* 305, 393-396.

Pubmed: [Author and Title](#)

CrossRef: [Author and Title](#)

Google Scholar: [Author Only](#) [Title Only](#) [Author and Title](#)

Evangelista, M., Zigmund, S., and Boone, C. (2003). Formins: signaling effectors for assembly and polarization of actin filaments. *Journal of Cell Science* 116, 2603-2611.

Pubmed: [Author and Title](#)

CrossRef: [Author and Title](#)

Google Scholar: [Author Only](#) [Title Only](#) [Author and Title](#)

Fischer-Parton, S., Parton, R.M., Hickey, P.C., Dijksterhuis, J., Atkinson, H.A., and Read, N.D. (2000). Confocal microscopy of FM4-64 as a tool for analysing endocytosis and vesicle trafficking in living fungal hyphae. *J Microscopy* 198, 246-259.

Pubmed: [Author and Title](#)

CrossRef: [Author and Title](#)

Google Scholar: [Author Only](#) [Title Only](#) [Author and Title](#)

Giraldo, M.C., and Valent, B. (2013). Filamentous plant pathogen effectors in action. *Nat. Rev. Micro.* 11, 800-814.

Pubmed: [Author and Title](#)

CrossRef: [Author and Title](#)

Google Scholar: [Author Only](#) [Title Only](#) [Author and Title](#)

Giraldo, M.C., Dagdas, Y.F., Gupta, Y.K., Mentlak, T.A., Yi, M., Martinez-Rocha, A.L., Saitoh, H., Terauchi, R., Talbot, N.J., and Valent, B. (2013). Two distinct secretion systems facilitate tissue invasion by the rice blast fungus *Magnaporthe oryzae*. *Nat. Commun.* 4, 1996.

Pubmed: [Author and Title](#)

CrossRef: [Author and Title](#)

Google Scholar: [Author Only](#) [Title Only](#) [Author and Title](#)

Guo, W., Grant, A., and Novick, P. (1999). Exo84p is an exocyst protein essential for secretion. *J Biol Chem* 274, 23558-23564.

Pubmed: [Author and Title](#)

CrossRef: [Author and Title](#)

Google Scholar: [Author Only](#) [Title Only](#) [Author and Title](#)

- Hall, T. (1999). BioEdit: a user-friendly biological sequence alignment editor and analysis program for Windows 95/98/NT. *Nucl. Acids Symp. Ser.* 41, 95.
Pubmed: [Author and Title](#)
CrossRef: [Author and Title](#)
Google Scholar: [Author Only Title Only Author and Title](#)
- Hamer, J.E., Howard, R.J., Chumley, F.G., and Valent, B. (1988). A mechanism for surface attachment in spores of a plant pathogenic fungus. *Science* 239, 288-290.
Pubmed: [Author and Title](#)
CrossRef: [Author and Title](#)
Google Scholar: [Author Only Title Only Author and Title](#)
- He, B., and Guo, W. (2009). The exocyst complex in polarized exocytosis. *Current Opin Cell Biol* 21, 537-542.
Pubmed: [Author and Title](#)
CrossRef: [Author and Title](#)
Google Scholar: [Author Only Title Only Author and Title](#)
- Irieda, H., Maeda, H., Akiyama, K., Hagiwara, A., Saitoh, H., Uemura, A., Terauchi, R., and Takano, Y. (2014). Colletotrichum orbiculare Secretes Virulence Effectors to a Biotrophic Interface at the Primary Hyphal Neck via Exocytosis Coupled with SEC22-Mediated Traffic. *The Plant Cell* 26, 2265-2281.
Pubmed: [Author and Title](#)
CrossRef: [Author and Title](#)
Google Scholar: [Author Only Title Only Author and Title](#)
- Jones, L.A., and Sudbery, P.E. (2010). Spitzenkörper, Exocyst, and Polarisome Components in Candida albicans Hyphae Show Different Patterns of Localization and Have Distinct Dynamic Properties. *Eukaryotic Cell* 9, 1455-1465.
Pubmed: [Author and Title](#)
CrossRef: [Author and Title](#)
Google Scholar: [Author Only Title Only Author and Title](#)
- Jose, M., Tollis, S., Nair, D., Mitteau, R., Velours, C., Massoni-Laporte, A., Royou, A., Sibarita, J-B., and McCusker, D. (2015). A quantitative imaging-based screen reveals the exocyst as a network hub connecting endo-and exocytosis. *Molec Biol Cell* (online early doi: 10.1091/mbc.E14-11-1527).
Pubmed: [Author and Title](#)
CrossRef: [Author and Title](#)
Google Scholar: [Author Only Title Only Author and Title](#)
- Kershaw, M.J., and Talbot, N.J. (2009). Genome-wide functional analysis reveals that infection-associated fungal autophagy is necessary for rice blast disease. *Proc Natl Acad Sci USA* 106, 15967-15972.
Pubmed: [Author and Title](#)
CrossRef: [Author and Title](#)
Google Scholar: [Author Only Title Only Author and Title](#)
- Khang, C.H., Berruyer, R., Giraldo, M.C., Kankanala, P., Park, S.Y., Czymmek, K., Kang, S., and Valent, B. (2010). Translocation of Magnaporthe oryzae effectors into rice cells and their subsequent cell-to-cell movement. *The Plant Cell* 22, 1388-1403.
Pubmed: [Author and Title](#)
CrossRef: [Author and Title](#)
Google Scholar: [Author Only Title Only Author and Title](#)
- Kleemann, J., Rincon-Rivera, L.J., Takahara, H., Neumann, U., Ver Loren van Themaat, E., van der Does, H.C., Hacquard, S., Stuber, K., Will, I., Schmalenbach, W., Schmelzer, E. and O'Connell R.J. (2012). Sequential delivery of host-induced virulence effectors by appressoria and intracellular hyphae of the phytopathogen Colletotrichum higginsianum. *PLoS Pathogens* 8: e1002643.
Pubmed: [Author and Title](#)
CrossRef: [Author and Title](#)
Google Scholar: [Author Only Title Only Author and Title](#)
- Köhli, M., Galati, V., Boudier, K., Roberson, R.W., and Philippsen, P. (2008). Growth-speed-correlated localization of exocyst and polarisome components in growth zones of Ashbya gossypii hyphal tips. *Journal of Cell Science* 121, 3878-3889.
Pubmed: [Author and Title](#)
CrossRef: [Author and Title](#)
Google Scholar: [Author Only Title Only Author and Title](#)
- Lamping, E., Tanabe, K., Niimi, M., Uehara, Y., Monk, B.C., and Cannon, R.D. (2005). Characterization of the Saccharomyces cerevisiae sec6-4 mutation and tools to create S. cerevisiae strains containing the sec6-4 allele. *Gene* 361, 57-66.
Pubmed: [Author and Title](#)
CrossRef: [Author and Title](#)
Google Scholar: [Author Only Title Only Author and Title](#)
- Leung, H., Borromeo, S., Bernardo, M.A., and Notteghem, J.L. (1988). Genetic analysis of virulence in the rice blast fungus Magnaporthe grisea. *Phytopathol.* 78, 1227-1233.
Pubmed: [Author and Title](#)
CrossRef: [Author and Title](#)
Google Scholar: [Author Only Title Only Author and Title](#)
- Novick, P., Ferro, S., and Schekman, R. (1981). Order of events in the yeast secretory pathway. *Cell* 25, 461-469.
Pubmed: [Author and Title](#)
CrossRef: [Author and Title](#)
Google Scholar: [Author Only Title Only Author and Title](#)

- Novick, P., Field, C., and Schekman, R. (1980).** Identification of 23 complementation groups required for post-translational events in the yeast secretory pathway. *Cell* 21, 205-215.
Pubmed: [Author and Title](#)
CrossRef: [Author and Title](#)
Google Scholar: [Author Only Title Only Author and Title](#)
- Novick, P., Medkova, M., Dong, G., Hutagalung, A., Reinisch, K., and Grosshans, B. (2006).** Interactions between Rabs, tethers, SNAREs and their regulators in exocytosis. *Biochemical Society Transactions* 34, 683-686.
Pubmed: [Author and Title](#)
CrossRef: [Author and Title](#)
Google Scholar: [Author Only Title Only Author and Title](#)
- Ntoukakis, V., Mucyn, T.S., Gimenez-Ibanez, S., Chapman, H.C., Gutierrez, J.R., Balmuth, A.L., Jones, A.M.E., and Rathjen, J.P. (2009).** Host Inhibition of a Bacterial Virulence Effector Triggers Immunity to Infection. *Science* 324, 784-787.
Pubmed: [Author and Title](#)
CrossRef: [Author and Title](#)
Google Scholar: [Author Only Title Only Author and Title](#)
- Oh, S.-K., Young, C., Lee, M., Oliva, R., Bozkurt, T.O., Cano, L.M., Win, J., Bos, J.I.B., Liu, H.-Y., van Damme, M., Morgan, W., Choi, D., Van der Vossen, E.A.G., Veeshouwers, V.G.A.A., and Kamoun, S. (2009).** In Planta Expression Screens of Phytophthora infestans RXLR Effectors Reveal Diverse Phenotypes, Including Activation of the Solanum bulbocastanum Disease Resistance Protein Rpi-blb2. *The Plant Cell* 21, 2928-2947.
Pubmed: [Author and Title](#)
CrossRef: [Author and Title](#)
Google Scholar: [Author Only Title Only Author and Title](#)
- Okada, S., Leda, M., Hanna, J., Savage, N.S., Bi, E., and Goryachev, A.B. (2013).** Daughter cell identity emerges from the interplay of Cdc42, septins, and exocytosis. *Developmental Cell* 26, 148-161.
Pubmed: [Author and Title](#)
CrossRef: [Author and Title](#)
Google Scholar: [Author Only Title Only Author and Title](#)
- Park, G., Xue, C., Zhao, X., Kim, Y., Orbach, M. and Xu, J.R. (2006).** Multiple upstream signals converge on the adaptor protein Mst50 in Magnaporthe grisea. *The Plant Cell* 18, 2822-2835.
Pubmed: [Author and Title](#)
CrossRef: [Author and Title](#)
Google Scholar: [Author Only Title Only Author and Title](#)
- Park, G., Xue, C., Zheng, L., Lam, S., and Xu, J.R. (2002).** MST12 regulates infectious growth but not appressorium formation in the rice blast fungus Magnaporthe grisea. *Molec Plant Microbe Interact* 15, 183-192.
Pubmed: [Author and Title](#)
CrossRef: [Author and Title](#)
Google Scholar: [Author Only Title Only Author and Title](#)
- Raymond, C.K., Pownder, T.A., and Sexson, S.L. (1999).** General method for plasmid construction using homologous recombination. *BioTechniques* 26, 134-138, 140-131.
Pubmed: [Author and Title](#)
CrossRef: [Author and Title](#)
Google Scholar: [Author Only Title Only Author and Title](#)
- Read, N.D. (2011).** Exocytosis and growth do not occur only at hyphal tips. *Mol Microbiol* 81, 4-7.
Pubmed: [Author and Title](#)
CrossRef: [Author and Title](#)
Google Scholar: [Author Only Title Only Author and Title](#)
- Riquelme, M. (2013).** Tip growth in filamentous fungi: a road trip to the apex. *Annu. Rev. Microbiol.* 67, 587-609.
Pubmed: [Author and Title](#)
CrossRef: [Author and Title](#)
Google Scholar: [Author Only Title Only Author and Title](#)
- Riquelme, M., Bartnicki-García, S., González-Prieto, J.M., Sánchez-León, E., Verdín-Ramos, J.A., Beltrán-Aguilar, A., and Freitag, M. (2007).** Spitzenkörper Localization and Intracellular Traffic of Green Fluorescent Protein-Labeled CHS-3 and CHS-6 Chitin Synthases in Living Hyphae of Neurospora crassa. *Eukaryotic Cell* 6, 1853-1864.
Pubmed: [Author and Title](#)
CrossRef: [Author and Title](#)
Google Scholar: [Author Only Title Only Author and Title](#)
- Riquelme, M., Bredeweg, E.L., Callejas-Negrete, O., Roberson, R.W., Ludwig, S., Beltran-Aguilar, A., Seiler, S., Novick, P., and Freitag, M. (2014).** The Neurospora crassa exocyst complex tethers Spitzenkörper vesicles to the apical plasma membrane during polarized growth. *Mol Biol Cell* 25, 1312-1326.
Pubmed: [Author and Title](#)
CrossRef: [Author and Title](#)
Google Scholar: [Author Only Title Only Author and Title](#)
- Ryder, L.S., Dagdas, Y.F., Mentlak, T.A., Kershaw, M.J., Thornton, C.R., Schuster, M., Chen, J., Wang, Z., and Talbot, N.J. (2013).** NADPH oxidases regulate septin-mediated cytoskeletal remodeling during plant infection by the rice blast fungus. *Proc Natl Acad Sci USA* 110, 3179-3184.
Pubmed: [Author and Title](#)
CrossRef: [Author and Title](#)
Google Scholar: [Author Only Title Only Author and Title](#)

Sagot, I., Klee, S.K., and Pellman, D. (2002). Yeast formins regulate cell polarity by controlling the assembly of actin cables. *Nature Cell Biol* 4, 42-50.

Pubmed: [Author and Title](#)

CrossRef: [Author and Title](#)

Google Scholar: [Author Only](#) [Title Only](#) [Author and Title](#)

Salminen, A., and Novick, P.J. (1989). The Sec15 protein responds to the function of the GTP binding protein, Sec4, to control vesicular traffic in yeast. *J Cell Biol* 109, 1023-1036.

Pubmed: [Author and Title](#)

CrossRef: [Author and Title](#)

Google Scholar: [Author Only](#) [Title Only](#) [Author and Title](#)

Sambrook, J., and Russell, D.W. (2000). *Molecular cloning : A Laboratory Manual*. 3rd ed. (Cold Spring Harbour Laboratory Press, New York, USA).

Pubmed: [Author and Title](#)

CrossRef: [Author and Title](#)

Google Scholar: [Author Only](#) [Title Only](#) [Author and Title](#)

Saunders, D.G.O., Aves, S.J., and Talbot, N.J. (2010). Cell Cycle-Mediated Regulation of Plant Infection by the Rice Blast Fungus. *The Plant Cell* 22, 497-507.

Pubmed: [Author and Title](#)

CrossRef: [Author and Title](#)

Google Scholar: [Author Only](#) [Title Only](#) [Author and Title](#)

Sheu, Y.J., Santos, B., Fortin, N., Costigan, C., and Snyder, M. (1998). Spa2p interacts with cell polarity proteins and signaling components involved in yeast cell morphogenesis. *Molec Cell Biol* 18, 4053-4069.

Pubmed: [Author and Title](#)

CrossRef: [Author and Title](#)

Google Scholar: [Author Only](#) [Title Only](#) [Author and Title](#)

Soanes, D.M., Chakrabarti, A., Paszkiewicz, K.H., Dawe, A.L., and Talbot, N.J. (2012). Genome-wide Transcriptional Profiling of Appressorium Development by the Rice Blast Fungus *Magnaporthe oryzae*. *PLoS Pathog* 8(2): e1002514.

Pubmed: [Author and Title](#)

CrossRef: [Author and Title](#)

Google Scholar: [Author Only](#) [Title Only](#) [Author and Title](#)

Songer, J.A., and Munson, M. (2009). Sec6p anchors the assembled exocyst complex at sites of secretion. *Mol. Biol. Cell*. 20, 973-982.

Pubmed: [Author and Title](#)

CrossRef: [Author and Title](#)

Google Scholar: [Author Only](#) [Title Only](#) [Author and Title](#)

Stalder, D., Mizuno-Yamasaki, E., Ghassemian, M., and Novick, P.J. (2013). Phosphorylation of the Rab exchange factor Sec2p directs a switch in regulatory binding partners. *Proceedings of the National Academy of Sciences* 110, 19995-20002.

Pubmed: [Author and Title](#)

CrossRef: [Author and Title](#)

Google Scholar: [Author Only](#) [Title Only](#) [Author and Title](#)

Steinberg, G. (2007). Hyphal Growth: a Tale of Motors, Lipids, and the Spitzenkörper. *Eukaryotic Cell* 6, 351-360.

Pubmed: [Author and Title](#)

CrossRef: [Author and Title](#)

Google Scholar: [Author Only](#) [Title Only](#) [Author and Title](#)

Sudbery, P. (2011a). Fluorescent proteins illuminate the structure and function of the hyphal tip apparatus. *Fungal Genet Biol* 48, 849-857.

Pubmed: [Author and Title](#)

CrossRef: [Author and Title](#)

Google Scholar: [Author Only](#) [Title Only](#) [Author and Title](#)

Sudbery, P.E. (2011b). Growth of *Candida albicans* hyphae. *Nat. Rev. Micro.* 9, 737-748.

Pubmed: [Author and Title](#)

CrossRef: [Author and Title](#)

Google Scholar: [Author Only](#) [Title Only](#) [Author and Title](#)

Sweigard, J., Chumly, F., Carrol, A., Farrall, L., and Valent, B. (1997). A series of vectors for fungal transformation. *Fungal Genet. Newsl.*, 52-55.

Pubmed: [Author and Title](#)

CrossRef: [Author and Title](#)

Google Scholar: [Author Only](#) [Title Only](#) [Author and Title](#)

Taheri-Talesh, N., Horio, T., Araujo-Bazan, L., Dou, X., Espeso, E.A., Penalva, M.A., Osmani, S.A., and Oakley, B.R. (2008). The tip growth apparatus of *Aspergillus nidulans*. *Mol Biol Cell* 19, 1439-1449.

Pubmed: [Author and Title](#)

CrossRef: [Author and Title](#)

Google Scholar: [Author Only](#) [Title Only](#) [Author and Title](#)

Talbot, N.J., Ebbole, D.J., and Hamer, J.E. (1993). Identification and characterization of MPG1, a gene involved in pathogenicity from the rice blast fungus *Magnaporthe grisea*. *The Plant Cell* 5, 1575-1590.

Pubmed: [Author and Title](#)

CrossRef: [Author and Title](#)

Google Scholar: [Author Only](#) [Title Only](#) [Author and Title](#)

TerBush, D.R., Guo, W., Dunkelbarger, S., and Novick, P. (2001). Purification and characterization of yeast exocyst complex. *Methods in Enzymology* 329, 100-110.

Pubmed: [Author and Title](#)

CrossRef: [Author and Title](#)

Google Scholar: [Author Only](#) [Title Only](#) [Author and Title](#)

TerBush, D.R., Maurice, T., Roth, D., and Novick, P. (1996). The Exocyst is a multiprotein complex required for exocytosis in *Saccharomyces cerevisiae*. *EMBO J* 15, 6483-6494.

Pubmed: [Author and Title](#)

CrossRef: [Author and Title](#)

Google Scholar: [Author Only](#) [Title Only](#) [Author and Title](#)

Thompson, J.D., Higgins, D.G., and Gibson, T.J. (1994). CLUSTAL W: improving the sensitivity of progressive multiple sequence alignment through sequence weighting, position-specific gap penalties and weight matrix choice. *Nucleic Acids Res.* 22, 4673-4680.

Pubmed: [Author and Title](#)

CrossRef: [Author and Title](#)

Google Scholar: [Author Only](#) [Title Only](#) [Author and Title](#)

Veneault-Fourrey, C., Barooah, M., Egan, M., Wakley, G., and Talbot, N.J. (2006). Autophagic Fungal Cell Death Is Necessary for Infection by the Rice Blast Fungus. *Science* 312, 580-583.

Pubmed: [Author and Title](#)

CrossRef: [Author and Title](#)

Google Scholar: [Author Only](#) [Title Only](#) [Author and Title](#)

Verdin, J., Bartnicki-Garcia, S., and Riquelme, M. (2009). Functional stratification of the Spitzenkorper of *Neurospora crassa*. *Mol Microbiol* 74, 1044-1053.

Pubmed: [Author and Title](#)

CrossRef: [Author and Title](#)

Google Scholar: [Author Only](#) [Title Only](#) [Author and Title](#)

Wiederkehr, A., Du, Y., Pypaert, M., Ferro-Novick, S., and Novick, P. (2003). Sec3p is needed for the spatial regulation of secretion and for the inheritance of the cortical endoplasmic reticulum. *Mol Biol Cell* 14, 4770-4782.

Pubmed: [Author and Title](#)

CrossRef: [Author and Title](#)

Google Scholar: [Author Only](#) [Title Only](#) [Author and Title](#)

Wilson, R.A., and Talbot, N.J. (2009). Under pressure: investigating the biology of plant infection by *Magnaporthe oryzae*. *Nature Rev Microbiol* 7, 185-195.

Pubmed: [Author and Title](#)

CrossRef: [Author and Title](#)

Google Scholar: [Author Only](#) [Title Only](#) [Author and Title](#)

Xu, J.R., and Hamer, J.E. (1996). MAP kinase and cAMP signaling regulate infection structure formation and pathogenic growth in the rice blast fungus *Magnaporthe grisea*. *Genes Dev* 10, 2696-2706.

Pubmed: [Author and Title](#)

CrossRef: [Author and Title](#)

Google Scholar: [Author Only](#) [Title Only](#) [Author and Title](#)

Zhao, X., Kim, Y., Park, G. and Xu, J.R. (2005). A mitogen-activated protein kinase cascade regulating infection-related morphogenesis in *Magnaporthe grisea*. *The Plant Cell* 17, 1317-1329.

Pubmed: [Author and Title](#)

CrossRef: [Author and Title](#)

Google Scholar: [Author Only](#) [Title Only](#) [Author and Title](#)